Plant Soil
https://doi.org/10.1007/s11104-024-06552-7

RESEARCH ARTICLE

Plant colonizers of a mercury contaminated site: trace metals and associated rhizosphere bacteria

Emanuela D. Tiodar · Cecilia M. Chiriac · Filip Pošćić · Cristina L. Văcar · Zoltan R. Balázs · Cristian Coman · David C. Weindorf · Manuela Banciu · Ute Krämer · Dorina Podar

Received: 16 October 2023 / Accepted: 9 February 2024

Abstract

Background and aims Mercury (Hg) contamination poses severe human and environmental health risks. We aimed to evaluate the colonization of Hg-contaminated sites by native plants and the prokaryotic composition of rhizosphere soil communities of the dominant plant species.

Methods A field study was conducted at a Hg-contaminated site in Romania. Metal concentrations in soil and plant samples were analyzed using portable X-ray fluorescence spectrometry. The prokaryotic composition of rhizosphere soil communities was determined through 16S rRNA amplicon sequencing and community functionality was predicted through PICRUSt2.

Results Site-specific trace metal distribution across the site drove plant species distribution in the highly contaminated soil, with *Lotus tenuis* and *Diplotaxis muralis* associated with higher Hg concentrations. In addition, for the bacterial communities in the rhizosphere soil of *D. muralis*, there was no observable decrease in alpha diversity with increasing soil Hg levels. Notably, Actinomycetota had an average of 24% relative abundance in the rhizosphere communities that also tested positive for the presence of *merA*, whereas in the absence of *merA* the phylum's relative abundance was approximately 2%. *merA* positive rhizosphere communities also displayed an inferred increase in ABC transporters.

Responsible Editor: Juan Barcelo.

Supplementary Information The online version contains supplementary material available at https://doi.org/10.1007/s11104-024-06552-7.

E. D. Tiodar · C. L. Văcar · Z. R. Balázs
Doctoral School of Integrative Biology, Babeș-Bolyai University, Cluj-Napoca, Romania

E. D. Tiodar · C. L. Văcar · Z. R. Balázs · M. Banciu · D. Podar (✉)
Centre for Systems Biology, Biodiversity and Bioresources (3B), Babeș-Bolyai University, Cluj-Napoca, Romania
e-mail: dorina.podar@ubbcluj.ro

C. M. Chiriac
Institute of Hydrobiology, Biology Centre CAS, České Budějovice, Czech Republic

F. Pošćić
Tucson, USA

Z. R. Balázs · M. Banciu · D. Podar
Department of Molecular Biology and Biotechnology, Babeș-Bolyai University, Cluj-Napoca, Romania

C. Coman
NIRDBS, Institute of Biological Research, Cluj-Napoca, Romania

D. C. Weindorf
School of Earth, Environment, and Sustainability, Georgia Southern University, Statesboro, GA, USA

U. Krämer
Department of Molecular Genetics and Physiology of Plants, Ruhr University Bochum, 44801 Bochum, Germany

Published online: 16 March 2024

Conclusions The results suggest a dependence of species-wise plant survival on local trace metal levels in soil, as well as an intricate interplay of the latter with rhizosphere bacterial diversity. Knowledge of these interdependencies could have implications for phytoremediation stakeholders, as it may allow for the selection of plant species and appropriate soil microbial inoculates with elevated Hg tolerance.

Keywords Tolerance · Phytoremediation · *Diplotaxis muralis* · *Lotus tenuis* · *Mercuric reductase* (MerA) · Gemmatimonadota

Introduction

Soil serves as an essential foundation of our natural world. It is a vital source of sustenance, supplying 95% of the food we rely on through the circulation and management of water, nutrients, and carbon-based resources (FAO 2022). Over 25% of the planet's biodiversity relies upon soil health. Beyond being a habitat, soil and soil-based products play substantial roles in our world economies (European Commission 2020). Consequently, European legislation proposals aimed at conserving the EU's natural capital have recognised the protection of soil as a worthy and profitable objective (European Commission 2019). For stakeholders interested in phytoremediation, the preservation of soil quality is of paramount importance towards sustainable and effective remediation outcomes. Finally, soil health touches directly on multiple sustainable development goals of the United Nations (2023) (e.g., 2: zero hunger; 3: good health and well-being; 6: clean water and sanitation; 11: sustainable cities and communities; 12: responsible consumption and production; 15: life on land).

Trace metals are a minor component of a soil's mineral composition. However, natural processes and human activities have caused many sites worldwide to exceed legal threshold concentrations for one or more trace metals such as mercury, lead (Pb), copper (Cu), zinc (Zn), and manganese (Mn) (Tchounwou et al. 2012). For example, an estimated 2.5 million metal-contaminated sites exist in the European Union, amounting to 28.3% of its land area (Panagos et al. 2013; Tóth et al. 2016). Industrial land use has left large, ecologically hazardous, untreated metal-polluted brownfields, exposing humans and food production to toxic elements via wind erosion and water leaching (Cundy et al. 2016; Ronchi et al. 2019). The substance priority risk of the agency for toxic substances and disease registry classifies the non-essential elements Pb and Hg, respectively, as the second and the third most toxic elements to human health (Abadin et al. 2020; ATSDR 2022a). Similarly, other trace metals such as Cu, Mn, and Zn, which have a physiological role as nutrients in cell metabolism at very low concentrations, also become toxic to organisms when present in excess (ATSDR 2005, 2013, 2022b). Hence, by referring to the globally established baseline average concentrations, we can assess the degree of metal contamination in the topsoil. These baselines differ strongly between elements. For example, total global topsoil Hg concentration averages at 0.4 mg kg^{-1} d.w., whereas the averages for Pb, Cu, Zn, and Mn are 25, 18, 64, and 437 mg kg^{-1} d.w., respectively (Kabata-Pendias 2011; Salminen et al. 2005). Concerning plant life, an imbalanced elemental composition within the tightly controlled network of plant cells and tissues can cause stress, cell death, and reduced biomass gain (Alloway 2013). Notably, the accumulation of trace metals in soil and plants can potentially result in progressive accumulation with increasing trophic level in the food web, thus enhancing human health risks. Accordingly, it is imperative to safeguard soils worldwide against excessive metal loading.

Strategies for managing contaminated brownfields aim to restore soil health for long-term ecosystem recovery (European Commission 2019). Phytoremediation is a sustainable green alternative to costly soil removal and consists of utilizing plants to restore brownfields (Liu et al. 2018; Mench et al. 2018). Phytoremediation has been explored as a strategy using plants alone, plants augmented with microorganisms or chemical compounds, or as complementary to other established technologies (Garbisu et al. 2020). Phytoremediation requires specific management of the contaminated fields (phytomanagement), however, as well as local fitness of the employed plants, which can be achieved through the use of locally adapted spontaneous plant communities (Garbisu et al. 2020). Characterizing the inherent tolerance strategies of native plants can provide relevant insights into the design of future phytomanagement trials.

A feasible phytomanagement of a metal-contaminated brownfield also considers the microorganisms

associated with plant roots (Borymski et al. 2018; Tiodar et al. 2021). Bacteria can play a vital role in assisting plants to colonize the site by contributing to the cycling of elements like N, P, and C, and by restoring soil properties to support micro- and macrofauna, thereby promoting a healthy ecosystem (Krausfeldt et al. 2017; Popendorf and Duhamel 2015; Wang et al. 2012). Microorganisms have also developed mechanisms that enable them to thrive in polluted sites. For example, bacteria can assist phytomanagement efforts for trace metals through their metal resistance mechanisms, such as the *mer* operon for Hg (Frossard et al. 2018). The *mer* operon is found across many bacterial phyla, and it contains genes encoding regulatory, uptake, and catalytic proteins. The main catalytic function of the *mer* operon is performed by a mercuric reductase (MerA) which reduces the highly reactive cationic form of mercury, Hg^{2+}, to the volatile, inert, monoatomic mercury vapour, Hg^0. Bacterial survival in environments that are contaminated with organic Hg is favoured by the presence of an organomercurial lyase (MerB) within the *mer* operon which catalyses the breakage of a C-Hg bond in highly toxic alkyl- and aryl-mercurial compounds, yielding CH_4 and Hg^{2+}, which is then reduced to Hg^0 by MerA (Nies and Silver 2007). These processes of bacterial Hg immobilization or volatilization are particularly important for soil health because they restructure soil biochemistry and locally ameliorate metal stress for plant roots (Borymski et al. 2018).

In Romania alone there are 177 registered anthropogenically contaminated sites, amassing 4101 km^2 of artificial surface (approximately 2% of the country's total surface) (Ministry of Energy 2022). In this exploratory field study, we focused on one industrially contaminated polymetallic site with Hg hotspots, where soil exceeds by far (Table 1) (Frenţiu et al. 2015; Văcar et al. 2021) the national limit of safety for total soil Hg (4 mg kg^{-1} d.w.) for industrial sites (Ministerial Order No. 756/1997, 1997). The aim of this study was to evaluate the degree to which the spontaneous flora and its associated rhizosphere bacteria have successfully colonized these patches of toxic substrate, and to assess its potential for remediation of Hg-contaminated soil. Specifically, the objectives of the study were to: (i) screen and identify plants growing at the Hg-contaminated site; (ii) identify plant species with high Hg accumulation potential; and (iii) characterize the diversity of bacterial communities residing in the rhizosphere soil of the dominant plant species. We hypothesized that the native flora developed tolerance by avoiding or accumulating toxic metals in order to colonize artificially uninhabitable grounds, and likewise, the rhizosphere bacterial communities have acquired their own resistance mechanisms.

Materials and methods

Study area and sample collection

The study site is located in Turda, Cluj County, Northwest Romania, on the grounds of a former chemical plant established in 1911 (Fig. 1). At the Turda Chemical Plant, chlorine (Cl_2), as well as sodium and potassium hydroxides (NaOH and KOH) were produced since 1958 through electrolysis of sodium chloride (NaCl) and potassium chloride (KCl)

Table 1 Total soil metal concentrations: minima, maxima, and median measured at the former chlor-alkali site in Turda, Romania. Legal limits for soil metal concentrations are given for Romania according to the Ministerial Order No. 756/1997, 1997. Values are in mg kg^{-1} d.w. ($n = 25$)

Summary statistics		Hg	Pb	Cu	Zn	Mn
Min [mg kg^{-1}]		33	36	27	137	866
Max [mg kg^{-1}]		2601	996	1167	3603	2314
Median [mg kg^{-1}]		962	350	261	388	1149
Sensitive soils legal limit [mg kg^{-1}]	Alert	1	50	100	300	1500
	Intervention required	2	100	200	600	2500
Industrial soils legal limit [mg kg^{-1}]	Alert	4	250	250	700	2000
	Intervention required	10	1000	500	1500	4000

Fig. 1 Map (Google Maps 2022) showing the location of the investigated site (Turda, Romania) and the subplots (T1 to T6) (marked by red dashed lines) used for the plant community survey of this study. The rectangle marked by yellow dashed lines depicts the area covered by the former building that nowadays consists mainly of large blocks of concrete. Within the sampling area, vegetation was present predominantly between the yellow and red lines

salts as primary materials. A total of 44 electrolysis cells lined with Hg cathodes were assembled inside the facility located within the industrial area (Maghear 2013). During the years of peak activity, Cu- and Zn-containing pesticides and calcium hypochlorite were also synthesized. Over >30 years of activity, tonnes of Hg were used, leaked through the basement of the building, and eventually accumulated in the ground underneath the cement of the facility or possibly leached into the surrounding environment including the Arieș River nearby (Prodan et al. 2011). In the late 90s the activity at the site ceased, facilities were partly demolished and abandoned, leaving behind metal and cement debris of the former building. According to the latest environmental report, the site was contaminated with 3.6 t of pure Hg and 1.5 t of Hg-containing waste (Cluj County Council 2012).

The area surveyed in this study consists of a 6000 m^2 surface of the industrial complex left after the demolition of the electrolysis facilities (N = 46.557192°, E = 23.781689°), which was further delimitated into six subplots (T1 to T6) (Fig. 1). The location has a warm and humid continental climate and is mostly covered in concrete debris; the margins of the area consist of Orthent soils that are heavily contaminated with metals (Table 1), as was previously characterized in Văcar et al. (2021). Previous studies have recorded a pH of 8.3, a median concentration of 11 g kg^{-1} for total organic carbon (TOC), and median concentrations, expressed in g kg^{-1}, of 12 for aluminium (Al), 66 for calcium (Ca), 0.05 for chloride (Cl), 24 for iron (Fe), 5 for potassium (K), 5 for magnesium (Mg), 1 for Mn, 1 for sodium (Na), 0.05 for nitrate (NO_3^-), and 0.3 for sulfate (SO_4^{2-}) (Frenţiu et al. 2015). The ecological hazard of Hg contamination is even more severe as the mobility of Hg increases. To understand the contamination profile at the site, 55 mg kg^{-1} of total Hg was previously characterized as mobile (6.8%), semi-mobile (76.7%) and non-mobile (11.3%) fractions (Frenţiu et al. 2015).

Plant community survey and collection of samples

In the summer of 2019, a plant community survey was conducted on the site according to Braun-Blanquet (1964), for which the sampling area was subdivided into six subplots (T1-T6) of approximately 1000 m^2 each (Fig. 1). The investigated subplots included the concrete debris of the former building (within the yellow grid (Fig. 1)), even though among the ruins, there were only very few plants. The following abundance scores were given for the plants found at the site: 0 = 0% coverage, r = single individuals, + = very few individuals, 1 = < 10% cover, 2a = 5–12% and 2b = 13–25% (Braun-Blanquet 1964; Mueller-Dombois and Ellenberg 1974). No species were found with a relative abundance >25%. Plant individuals were sampled in accordance with their proportional abundance at the site (Table 2). The plants were excavated to maximally protect their root system then shaken manually for a few seconds to discard the loosely attached soil from the roots. Each plant was separated into root and shoot, placed in individual plastic bags and put on ice for transport to the laboratory. Shoots were carefully washed under running water and then several times with distilled water to remove any potential dust deposited on the leaves. Roots were processed as follows in order to collect both the rhizosphere soil and the root tissues. Rhizosphere soil refers to the soil closely adhering to the roots. The adhering soil was detached from the roots by gloved-hand or plastic scrapers. Rhizosphere soil collected from three individual plants growing within a 50 cm radius was pooled to form one rhizosphere soil sample used for metal analysis. After detaching the rhizosphere soil, the roots of each individual plant were carefully washed under running water and then several times with distilled water to further remove the remaining soil particles. For the microbial diversity analysis, a small fraction of the pooled rhizosphere soil of *D. muralis* plants collected for metal analysis was stored at −80 °C for later DNA extraction. At the time of sampling, *D. muralis* was at the pre-flowering stage.

Analysis of metal contents

To prevent Hg loss via volatilization, soil and washed root and shoot samples were air-dried at room temperature (20–21 °C) for six days. Subsequently, soil and plant samples were ground into a fine powder using agate and porcelain mortars and pestles, respectively. Total Cu, Hg, Mn, Pb, and Zn were quantified in solid samples using a portable X-ray fluorescence (pXRF) spectrometer (Vanta series, Olympus, Waltham, MA, USA) (Supplementary Table 1) (Weindorf and Chakraborty 2020). Briefly, dry powder samples were set in a thin layer onto a Prolene thin film that covered the aperture of the instrument. The pXRF device was placed on a flat surface and used in a portable test stand configuration, being operated on a line power (115 VAC) at 10–40 keV. Using *Geochem Mode*, each sample was sequentially scanned with three beams with a dwell time of 45 s per beam. Prior to sample measurement, instrument calibration was performed with a '316' stainless steel alloy. The raw concentration values of Cu, Hg, Mn, Pb, and Zn in soil and plant tissues were corrected by applying correction factors based on the values of the reference materials that were added to each sample measurement cycle (NIST 2711a-Montana II soil and NIST 1515-Apple leaves) following the formula from Koch et al. 2017. The recovery percentages of the pXRF

Table 2 Plant species and their spread across the industrial site of the former chlor-alkali plant; n = number of samples taken from the field. The adapted abundance scores given were: 0 = 0% coverage, r = single individuals, + = very few individuals, 1 = < 10% cover, 2a = 5–12% and 2b = 13–25% (Braun-Blanquet 1964; Mueller-Dombois and Ellenberg 1974)

Plant species	Family	Primary Growth Form	Present at subplot	Adapted Braun-Blanquet coefficient	*n*
Diplotaxis muralis (L.) DC.	Brassicaceae	herb	1, 2, 3, 4, 5, 6	2b	27
Lotus tenuis Waldst. & Kit. ex Willd.	Fabaceae	herb	1, 2, 4, 5, 6	2a	15
Calamagrostis epigejos (L.) Roth	Poaceae	grass	1, 2, 4, 5	2a	15
Erigeron annuus (L.) Pers.	Asteraceae	herb	1, 3, 6	1	12
Plantago lanceolata (L.)	Plantaginaceae	herb	6	+	3
Tussilago farfara (L.)	Asteraceae	herb	4	+	3

measurement for the five elements of interest determined for the reference materials are given in Supplementary Table 2. Cu, Hg, Pb, and Zn concentrations in the rhizosphere soil samples used for DNA extraction were quantified by inductively-coupled plasma mass spectrometry (ICP-MS, Perkin-Elmer Elan DRC II) upon microwave acid digestion (Multiwave Go Plus, Anton Paar) in Teflon vessels with aqua regia (HNO_3:HCl = 1:3 (v:v)). NIST 2711a-Montana II soil was included among the samples to assess technical accuracy during digestion and ICP measurements. The recovery percentages are given in Supplementary Table 2.

Microbial biodiversity and prediction-based functional analysis associated with the rhizosphere soil of the dominant plant species

The rhizosphere soil biodiversity of *Diplotaxis muralis* (the most abundant plant species at the site) was explored using a metabarcoding approach. Total DNA was extracted in triplicates using a Quick-DNA Fecal/Soil Microbe Miniprep Kit (#D60010 ZYMO Research, USA) following the manufacturer's instructions. The three technical replicates of the total DNA samples were pooled, and the DNA concentration was measured with a Nanodrop spectrophotometer (ThermoFisher Scientific, USA), before continuing with library preparation for the sequencing step. The V3-V4 regions of the 16S rRNA gene were amplified using the PRK341F/PRK806R primers modified by addition of Illumina-specific adaptors. The sequencing step was performed on a MiSeq platform (Illumina, USA) using V3 sequencing chemistry with 300 bp paired-end reads. Raw sequence data was processed as described in detail in Chiriac et al. (2017) and Szekeres et al. (2018). Sequence data generated in this study have been deposited in the European Nucleotide Archive (ENA) at EMBL-EBI under project accession numbers PRJEB67299.

The Phylogenetic Investigation of Communities by Reconstruction of Unobserved States (PICRUSt) algorithm was used to infer potential biological functions to the 16S rRNA gene-based microbial diversity profiles based on predicted metagenomes (Langille et al. 2013). The FASTA sequence files and the normalized biom table of OTUs (QIIME output) were loaded into the PICRUSt2 (ver. 2.5.2) pipeline, using the default parameters. The resulted pred_metagenome_unstrat.tsv table with the gene family counts per sample annotated via the Kyoto Encyclopedia of Genes and Genomes (KEGG) Orthology (KO) gene database was further imported into R (R Core Team 2023). The *ggpicrust2* package was used to map and summarize the KO genes to predicted KEGG path-way-level categories and to generate a principal component analysis (PCA) via the pathway_pca() function (Yang et al. 2023). Next, the count data was converted to relative abundance per sample and was used for visualizing the most abundant level 1, 2 and 3 KEGG pathways imputed for the environmental samples.

Endpoint PCR for *merA* gene

The presence of the *mercuric reductase* (*merA*) gene in the rhizosphere soil total DNA was assessed using endpoint PCR amplification. Degenerated *merA* specific primers (A2-n.F and A5-n.R), as specified in Liu et al. (2012), and DreamTaq Green PCR Master Mix (2X) (ThermoFisher Scientific #1081) were used to generate a fragment of 1250 bp under the following PCR conditions: 5 min at 95 °C initial denaturation, followed by 35 cycles of 40 seconds at 95 °C, 40 seconds at 56 °C, and 1 minute 30 seconds at 72 °C. Thirty ng of soil total DNA was used as template. The resulting amplicons were separated on a 1% (w/v) agarose gel.

Data analyses and statistics

An ecological risk index of the site was generated for the elements of interest in this study (Hakanson 1980). Natural background contents of the upper continental crust were used as pre-industrial baseline values (Taylor and McLennan 1995; Gustin et al. 1999). For the elemental concentration data, values below the instrument limit of detection (LOD) were replaced by $LOD \times 2^{-0.5}$ (Hornung and Reed 1990). Using the metal concentrations, the following coefficients were determined: bioaccumulation (BAF), calculated as the quotient of the metal concentration in shoot and in the rhizosphere soil, bioconcentration (BCF), the quotient of the metal concentration in root and in the rhizosphere soil, and translocation (TF), the quotient of metal concentration in shoot and root (Ruiz-Huerta et al. 2022; Zanganeh et al. 2022). Statistical analysis was conducted with one-way analysis

of variance (ANOVA). A posteriori comparisons of means was performed using Tukey's test based on the minimum significant difference (MSD) method obtained from the T′ statistics for unequal sample sizes (Sokal and Rohlf 2012). Data were subjected to logarithmic transformation prior to analysis, which effectively homogenized the variances (Levene's test) and produced normal distributions (Shapiro-Wilk test, normal probability plots, and visual histogram distribution) (Sokal and Rohlf 2012). Consequently, the median values were used instead of the arithmetic means. The relationships between the concentrations of elements in soil and plant organs were tested using Pearson correlation coefficients (bivariate correlation with two-tailed testing) (Sokal and Rohlf 2012). The responses of root and shoot Hg to soil Hg levels, and the responses of shoot Hg to root Hg were analysed at the species level using the test for equality of the regression coefficients (slopes) of several regression lines (Sokal and Rohlf 2012). Furthermore, redundancy analysis (RDA) (Podani 2000) was undertaken using metal concentrations in both roots and shoots, along with plant species (included as dummy variable), as response variables. For the explanatory variables, z-scores of the log-transformed soil metal concentrations were used, incorporating all available variables (i.e. employing a full model approach). The RDA model was validated using an ANOVA test with 999 permutations (Supplementary Table 3). The main R script used to prepare the data and generate the model was adapted from Borcard et al. (2012) and Zuur et al. (2007). The base and vegan (ver. 2.6–4) (Oksanen et al. 2017) R packages were used for ANOVA and RDA analysis, respectively.

Results

Plant species distribution

Within the whole perimeter of the former chlor-alkali plant, only several herbaceous plant species were present and they were identified as members of Brassicaceae, Fabaceae, and Poaceae families (Table 2). The dominant species, present throughout most of the area were *Diplotaxis muralis*, *Lotus tenuis*, and *Calamagrostis epigejos* (Fig. 2). *Erigeron annuus*, *Plantago lanceolata* and *Tussilago farfara* were present only occasionally.

Metal concentrations across the soil – plant system

Mercury

Median Hg concentrations were similar in the rhizosphere soils of *L. tenuis*, *D. muralis*, *E. annuus*, and *P. lanceolata* (Fig. 3A), and between two- and ten-fold higher than in those of *C. epigejos* and *T. farfara*. Albeit not statistically significant in all cases, *L. tenuis* displayed the highest median Hg concentrations of 1200, 5425, and 637 mg kg^{-1} in the rhizosphere soil, root and shoot, respectively. The extent to which the six plant species accumulated Hg in root varied substantially, with a ration of the highest to the lowest median concentration between 3 and 3850. However, the median shoot Hg concentrations in all the other plant species were only 2 to 7 times lower than that of *L. tenuis*. Overall, root Hg concentrations were higher than shoot concentrations in the majority of plant species. The plant species deviating from this general observation were *P. lanceolata* and *T. farfara*, for which the shoot concentrations were higher than those in the root by 3 and 63 times, respectively. *E. annuus* had the lowest bioaccumulation (BAF) and translocation (TF) coefficients of all plant species (Fig. 4A). Bioconcentration (BCF) and TF coefficients >1 were observed, and *D. muralis* had the highest percentage of individuals with BCF >20 (11%) and TF >1 (22%). Possibly, collection of the largest number of individuals for this plant species led to a large variability in soil Hg concentration, and consequently in the foliar Hg accumulation, but also increased the chances of picking up individuals with high tissue Hg concentrations.

Lead

The highest rhizosphere soil median Pb concentration (402 mg kg^{-1}) was observed for *P. lanceolata*, with no significant differences amongst the plant species. *Calamagrostis epigejos* accumulated the highest median Pb concentration in roots (117 mg kg^{-1}), the value being 1.6 to 23 times greater than for the other plant species (Fig. 3B). For shoot Pb concentration, the highest median was 46.5 mg kg^{-1}, for *P. lanceolata*, and was 5 to 3 times and significantly higher than for the remaining plant species (Fig. 3B). BAF and BCF coefficients were largely below 0.5 and 1, respectively (Fig. 4B). Median TF coefficients >1

Fig. 2 Plant individuals found at the Turda site for the first two most abundant species: *Diplotaxis muralis*, in the T2 (**A**) and *Lotus tenuis* in T5 (**B**) subplots

were recorded for both *T. farfara* and *P. lanceolata*. Although the median TF coefficient for *D. muralis* was <1, 37% of individuals displayed TF above unity.

Copper

Most plant species displayed similar median Cu concentrations in their rhizosphere soils, with overlapping interquartile ranges, except for *T. farfara*, which grew on a patch with the lowest Cu concentration (27 mg kg^{-1}) (Fig. 3C). In roots, *C. epigejos* accumulated the highest median Cu concentration (365 mg kg^{-1}), which was 2 to 14 times higher than in the other plant species. In shoots, Cu concentrations were similar across species, with about a two-fold higher median (71 mg kg^{-1}) in *P. lanceolata* than the lowest in *D. muralis* (34 mg kg^{-1}). The highest BAF, BCF, and TF coefficients were observed for *T. farfara*. BCF coefficients >1 were also observed in 40% of *C. epigejos* individuals, 33% of *E. annuus* individuals, and 10% of the *D. muralis* individuals. Apart from *T. farfara*, the only other species with TF coefficients above unity was *D. muralis* (22% individuals) (Fig. 4C).

Zinc

The median Zn concentrations in rhizosphere soil ranged from 154 to 669 mg kg^{-1}, with the highest value (3600 mg kg^{-1}) recorded for *P. lanceolata* (Fig. 3D). In roots, median Zn concentration was highest in *C. epigejos* (436 mg kg^{-1}) and was 1.2 to 10 times higher than in the other plant species. Out of the six plant species, shoot Zn concentrations were highest in *P. lanceolata* (204 mg kg^{-1}), twice the lowest value of 84 mg kg^{-1} found in *D. muralis*. *Tussilago farfara* displayed values >1 for the BAF and TF coefficients (Fig. 4D). BCF coefficients >1 were not unusual, with 52%, 33%, and 17% of *D. muralis*, *C. epigejos*, and *E. annuus* individuals reaching this threshold, respectively.

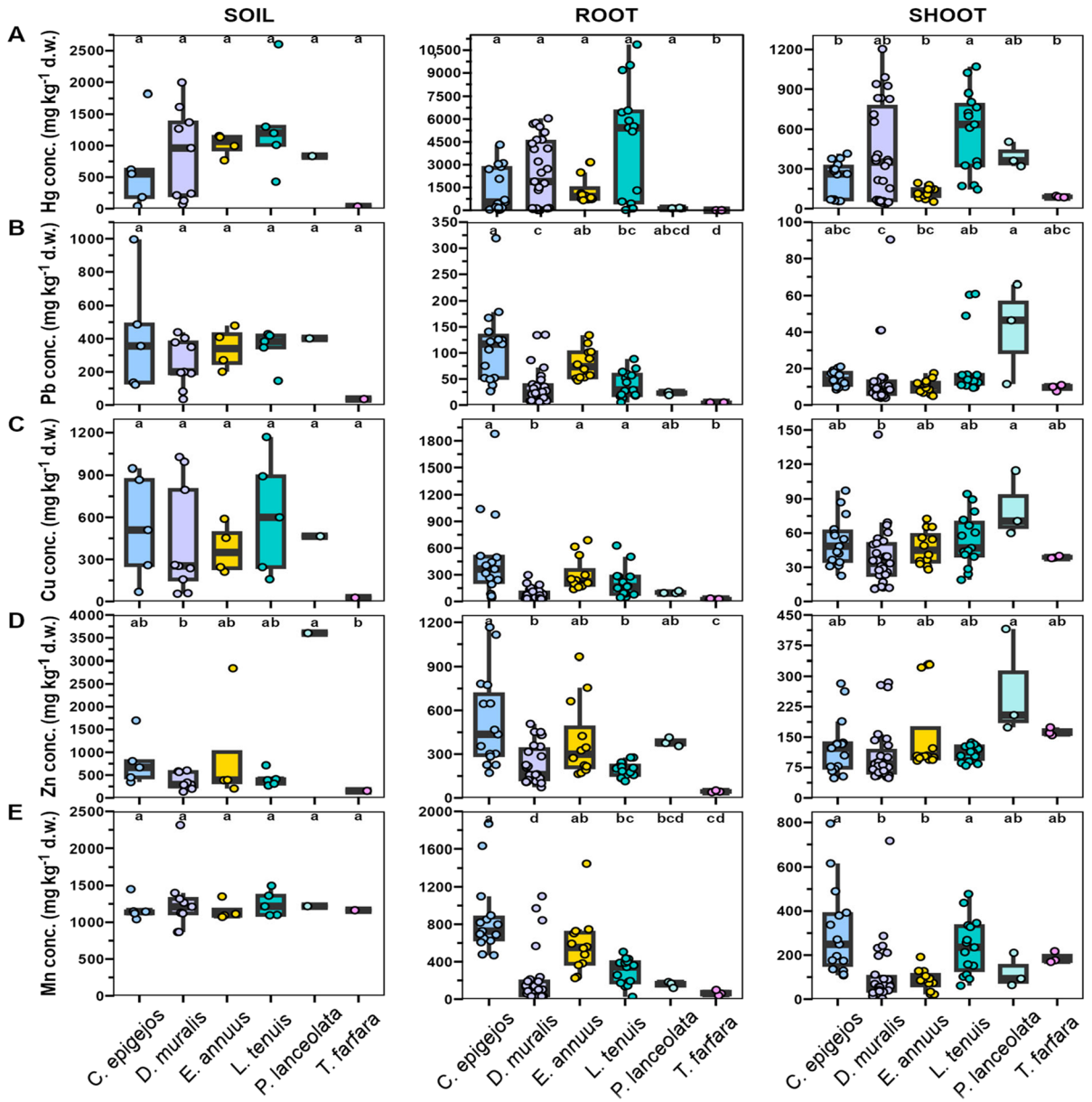

Fig. 3 Total metal concentrations in rhizosphere soil and plants at the sampling site in Turda, Romania. Boxplots showing Hg (**A**), Pb (**B**), Cu (**C**), Zn (**D**) and Mn (**E**) concentrations (mg kg^{-1} d.w.) determined for the rhizosphere soil (n = 1 to 9), root and shoot (n = 3 to 27) for the six plant species identified at the site (*Calamagrostis epigejos*, *Diplotaxis muralis*, *Erigeron annuus*, *Lotus tenuis*, *Plantago lanceolata*, and *Tussilago farfara*). Different characters indicate significant differences among the species for each element ($p \leq 0.05$, Tukey's test for unequal numbers of replicates). The line inside the box shows the median value. The box shows the range from first to third quartile (interquartile range, IQR) and the whiskers show the lowest/highest values within 1.5 IQR of the lower/upper quartile. Whiskers are not shown if the lower/upper quartile was equal to the lowest/highest value (excluding outliers). Individual data are presented as circles, and outliers are defined as data outside the whiskers. Conc. = concentration

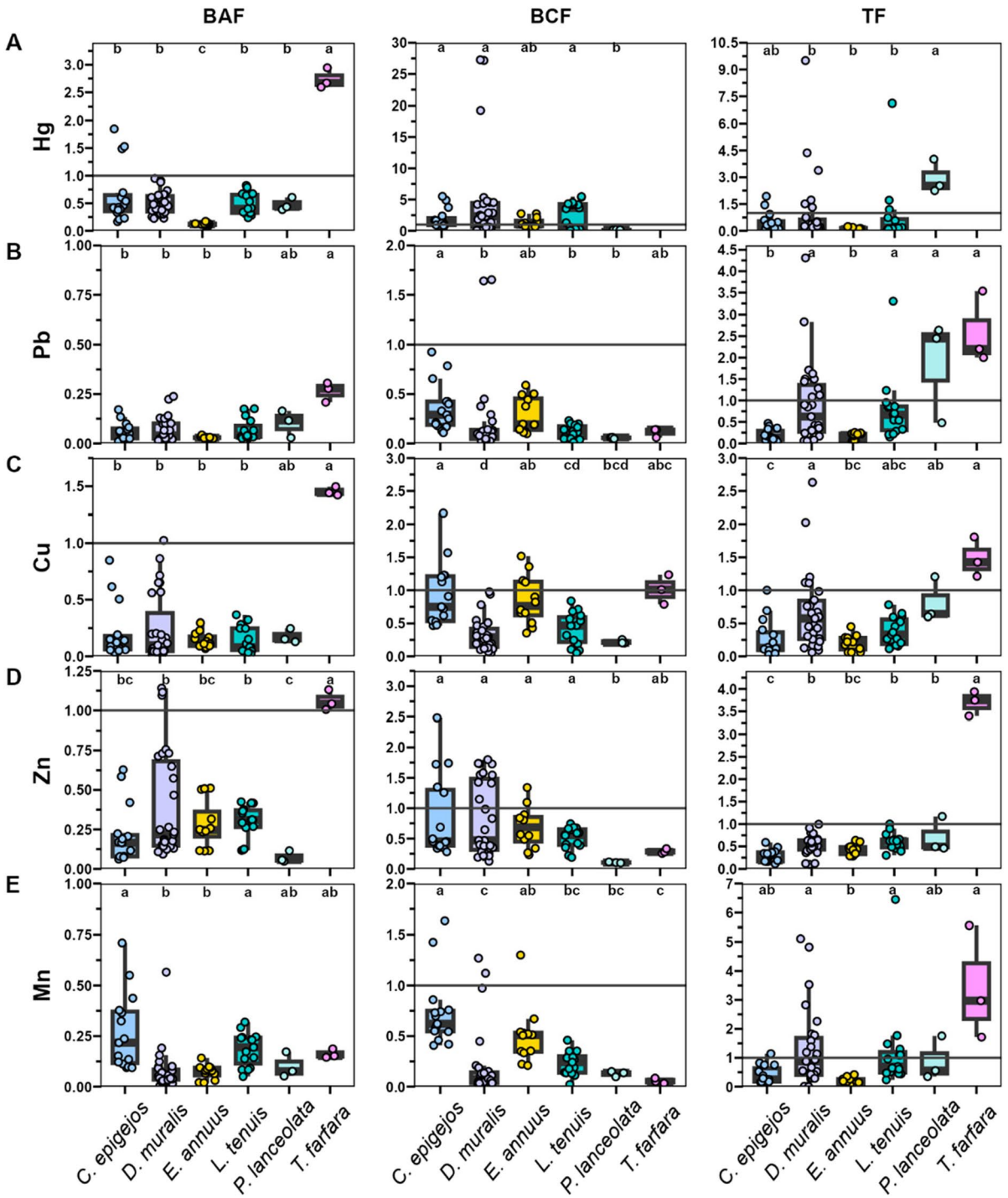

Manganese

Manganese concentration ranges were similar across the rhizosphere soils of all six plant species, with medians of ~1200 mg kg^{-1} (Fig. 3E). In both roots and shoots of *C. epigejos*, median Mn concentrations of 727 and 246 mg kg^{-1}, respectively, were the highest. Compared to other species, these concentrations

◂**Fig. 4** Plant metal accumulation coefficients for samples from Turda, Romania. Boxplots showing the Hg (**A**), Pb (**B**), Cu (**C**), Zn (**D**), and Mn (**E**) bioaccumulation ($BAF = [Metal]_{shoot}/[Metal]_{soil}$), bioconcentration ($BCF = [Metal]_{root}/[Metal]_{soil}$), and translocation ($TF = [Metal]_{shoot}/[Metal]_{root}$) factors ($n = 3$ to 27) for the six plant species identified at the site *(Calamagrostis epigejos, Diplotaxis muralis, Erigeron annuus, Lotus tenuis, Plantago lanceolata, Tussilago farfara)*. Grey horizontal lines show the plant accumulator threshold of these factors, equal to 1. Different characters indicate significant differences among the species for each element ($p \leq 0.05$, Tukey's test for unequal numbers of replicates). The line inside the box shows the median value. The box shows the range from first to third quartile (interquartile range, IQR) and the whiskers show the lowest/highest values still within 1.5 IQR of the lower/upper quartile. Whiskers are not shown if the lower/upper quartile was equal to the lowest/highest value (excluding outliers). Individual data are presented as circles, and outliers are defined as data outside the whiskers

were up to 12-fold, and 4-fold higher in roots and shoots, respectively. Manganese BAF and BCF were generally low, with values of <0.5 and 1, respectively (Fig. 4E). The highest median TF of 3 was observed for *T. farfara*, whereas median TF was below unity for all other plant species, except for ~44% of *D. muralis* and 47% of *L. tenuis* specimens.

The ranges of rhizosphere soil Hg concentrations differed substantially between species, with the largest range for *D. muralis* and the smallest range for *T. farfara*, for which the range of rhizosphere soil concentrations were comparably narrow also for Pb and Cu. Compared to soil, overall, there was a Hg enrichment in roots, but not of other metals in the plant species that were abundant at the sampling site. Root-to-shoot translocation of Hg and Pb was more efficient in *P. lanceolata* than in the other species. The highest TF coefficients for Pb, Cu, Zn, and Mn were found in *T. farfara*, although it represented the lowest number of individuals.

Soil – plant metal relationships

Relationships between metal concentrations in rhizosphere soil and in plants were analysed only for the four species for which the relative abundance at the sampling site was >10% (Table 2). For Hg, the main contaminant at the site, significant positive correlations between the concentration of the metal in rhizosphere soil and in plant organs were established for the most abundant species *C. epigejos*, *D. muralis*, and *L. tenuis.* Whereas for *E. annuus*, although positive correlations were still observed, the correlation between Hg concentration in rhizosphere soil and in shoots was the only one statistically significant (Table 3). However, *E. annuus* was the sole species to display significant correlations at all levels investigated, for Pb and Zn (Table 3).

All plant species showed significant coefficients of determination (R^2), for all three relationships tested, except *E. annuus* (Fig. 5). Furthermore, the slopes were significantly different between species for the dependence of both root and shoot Hg concentrations on those in soil. For root Hg concentrations in relation to those in soil, the slope was maximal for *L. tenuis* and significantly different from all other species. Relative to soil Hg concentrations, shoot Hg concentrations increased most sharply in *E. annuus*, followed by *D. muralis* and *L. tenuis*, and were significantly different from *C. epigejos*. There were no significant differences between species in the slopes of regression lines of shoot Hg concentrations on root Hg concentrations (Fig. 5B).

Plant – soil interaction analysis

In a redundancy analysis (RDA, Fig. 6), soil Hg, Zn, Pb, Cu, and Mn, explained 13.1% ($p \leq 0.001$), 9.4% ($p \leq 0.001$), 5.5% ($p \leq 0.001$), 4.4% ($p \leq 0.001$), and 2.7% ($p \leq 0.01$), respectively, of the constrained variance (i.e. 35% of the total observed variance) in plant species distribution and shoot and root metal concentrations (Supplementary Table 4). The first two canonical RDA axes explained 76.5% of the constrained variance (Fig. 6). Together, Hg, Pb, Cu, and Zn explained mostly the first canonical axis, while Mn contributed to the explanation of the second canonical axis. Elevated root and shoot Hg concentrations were associated with elevated soil Hg. There was a positive association of Zn concentrations in roots, but not in shoots, with soil Zn. According to RDA, root and shoot Mn concentrations were positively associated with soil Mn, whereas plant Pb and Cu concentrations were not dependent on the respective soil metal. Additionally, soil Mn was positively associated with root and shoot Pb concentrations, root Zn, and shoot Cu concentrations.

The soil metals separated the plant community at the Turda site in two main directions: Hg, Pb, and Cu defined the first group of nonessential (Hg and Pb) or potentially toxic (Cu), whereas the essential

Table 3 Pearson correlation coefficient (r) between metal log-transformed concentrations in rhizosphere soil, root and shoot of *Calamagrostis epigejos* ($n=15$ plant; $n=5$ soil samples), *Diplotaxis muralis* ($n=27$ plant; $n=9$ soil samples), *Erigeron annuus* ($n=12$ plant; $n=4$ soil samples), and *Lotus tenuis* ($n=15$ plant; $n=5$ soil samples) for samples from Turda, Romania; in bold significant r values

Species		Hg	Pb	Cu	Zn	Mn
Calamagrostis epigejos	Soil vs. Root	**0.93*****	**0.64***	**0.89*****	0.24	0.10
	Soil vs. Shoot	**0.89*****	0.07	0.29	0.06	−0.46
	Root vs. Shoot	**0.93*****	−0.14	0.05	**0.61***	0.05
Diplotaxis muralis	Soil vs. Root	**0.69*****	0.25	**0.71*****	−0.29	−0.18
	Soil vs. Shoot	**0.94*****	**0.39***	−0.09	−0.36	**0.66*****
	Root vs. Shoot	**0.70*****	0.03	0.02	**0.44***	−0.32
Erigeron annuus	Soil vs. Root	0.38	**−0.73****	**0.58***	**0.90*****	0.33
	Soil vs. Shoot	**0.94*****	**0.92*****	0.35	**0.95*****	**0.59***
	Root vs. Shoot	0.40	**−0.59***	−0.31	**0.89*****	0.22
Lotus tenuis	Soil vs. Root	**0.90*****	0.19	0.42	0.08	0.37
	Soil vs. Shoot	**0.79*****	0.19	0.06	−0.44	**0.60***
	Root vs. Shoot	**0.93*****	0.37	**0.62***	0.08	0.38

* $p \leq 0.05$; ** $p \leq 0.01$; *** $p \leq 0.001$

micronutrients Zn and Mn summarized the second group. The main plant populations that preferred the toxic metals group were *L. tenuis*, followed by *D. muralis* (Fig. 6). The Zn-Mn group influenced the acquisition of Mn and Zn in root and the accumulation of Mn, Cu, and Pb in shoot (Fig. 6). The main plant populations distributed in this second group were *C. epigejos*, and *P. lanceolata*, while *E. annuus* remained between the two groups. However, *T. farfara* displayed an antagonistic relationship with all investigated soil metals and a low colonizing potential under higher Hg-Pb-Cu soil concentrations (Fig. 6).

Bacterial biodiversity in the rhizosphere soil of *Diplotaxis muralis*

Bacterial alpha diversity (within-sample diversity) in the rhizosphere soil of *D. muralis* was generally high, with the Shannon diversity index ranging from 5 to 8.2 (Table 4), and did not gradually decrease with increasing soil Hg concentration between 128 and 615 mg kg^{-1} (no significant correlations for alpha diversity metrics and Hg concentration; Supplementary Table 5). Median species richness based on the number of observed OTUs was 754, with a minimum of 173 in sample T_5, four times lower than the median (Table 4). The total estimated richness showed a similar trend, with a median Chao1 estimator of 787, three times lower in sample T_5. Conversely, a maximum of 904 observed OTUs and the highest Chao1 diversity index were observed in the T_1 soil sample containing the lowest Hg and Zn as well as, moderate Cu and Pb concentrations. However, the highest sample diversity (Shannon diversity index) was associated with elevated soil Hg concentrations closer to the median.

A Bray-Curtis based beta-diversity analysis supported the distinct community composition of the T_5 sample, and identified the highest similarity between the T_1 and T_6 samples (Fig. 7). Next, possible genetic elements conferring Hg resistance were evaluated. Total genomic DNA of all samples, except T_5, contained the *merA* gene (Fig. 7C).

Overall, the Pseudomonadata phylum was dominant, with ~50% relative abundance in all samples (Fig. 7A). The second most abundant phylum was Actinomycetota, with proportions between 19 and 30%, except for the T_5 sample, in which the relative abundance of Actinomycetota was 1.5% and the relative abundance of Gemmatimonadata was above 30%, much higher than in all other samples. Chloroflexota was of low abundance in T_5 (0.4%), but noteworthy in the other samples ranging from 3.6% to 7.3%. Acidobacteriota was more evenly distributed among samples, with relative abundances of 6.5% to 10.1%.

The most abundant phylotype belonged to the Gemmatimonadota phylum, but was not determined at the genus level. *Kaistobacter* was the second most abundant genus and was ubiquitously present in all

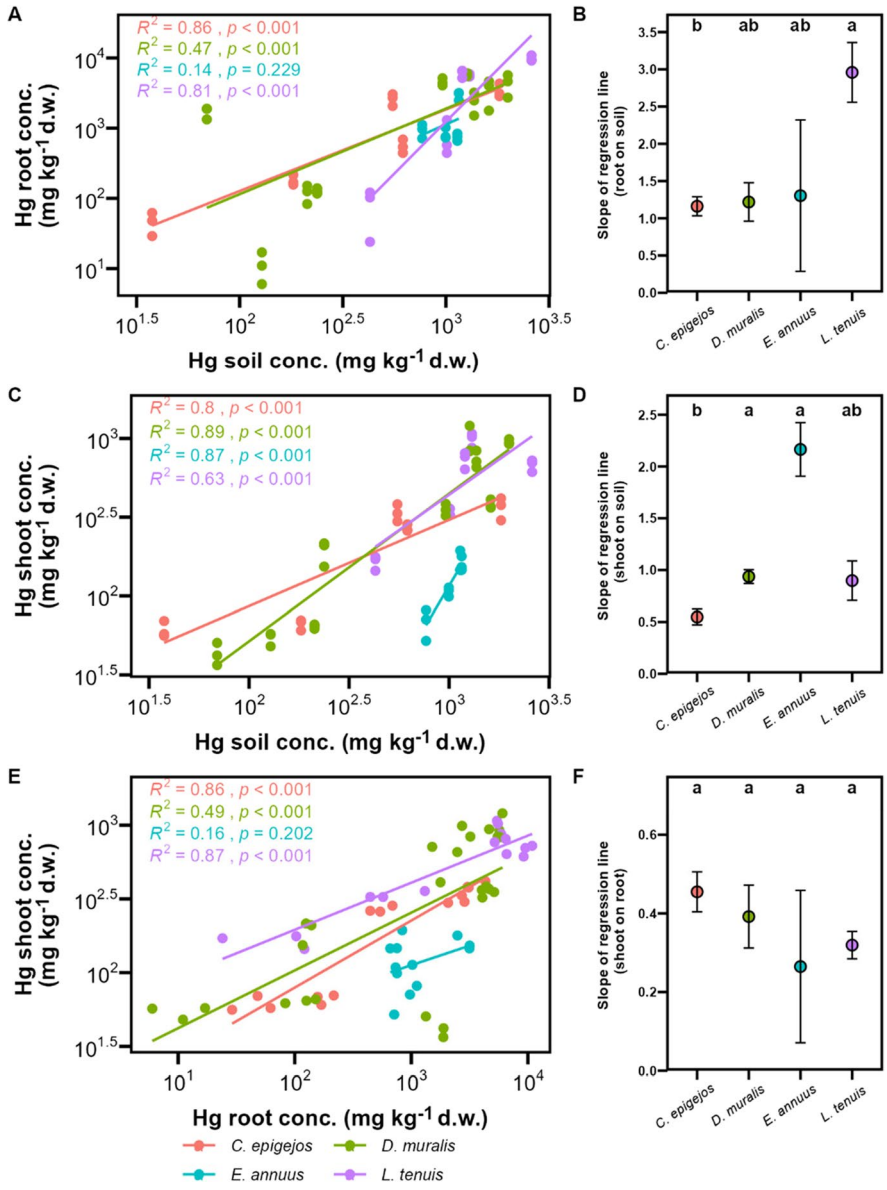

Fig. 5 Simple linear regression models and coefficients for Hg concentrations in rhizosphere soil and plants from Turda, Romania. Regression models for root on soil (**A**), shoot on soil (**C**), and shoot on root (**E**) Hg concentrations at the species level (*Calamagrostis epigejos*, *Diplotaxis muralis*, *Erigeron annuus*, and *Lotus tenuis*) with the corresponding regression coefficients of determination (R^2) and their significance (p value), for $n = 12$ to 27. Data are presented as log-log on a power function. The corresponding regression coefficients (slopes) and their standard error (SE) are shown in B, D, and F. Different lowercase letters indicate significant differences among slopes ($p \leq 0.05$, Tukey's-test for unequal numbers of replicates). Conc. = concentration

rhizosphere soil samples (Supplementary Fig. 2). Other noteworthy genera were *Mesorhizobium*, *Azospirillum*, *Pseudomonas*, *Paenibacillus*, *Bacillus*, and *Agrobacterium*, which were less prevalent and were present in low proportions (<0.01%).

Functional diversity of bacteria in the rhizosphere soil of *Diplotaxis muralis*

To infer potential functionality to the identified 16S rRNA gene-based microbial diversity data, the PICRUSt2 algorithm was used to predict the metagenomic content. The functional pathways determined were arranged via the KEGG pathways database in a three-level hierarchy. In total, there were 248 KEGG pathways (level 3 classification) predicted for the six *D. muralis* rhizosphere communities, as can be partially observed in Supplementary Table 6. The relative abundance of the level one KEGG pathways were similar across the six soil samples (Fig. 8A). The predominant functional pathway putatively employed by the microbial communities was metabolism with 70% mean relative abundance, followed by genetic information processing (mean

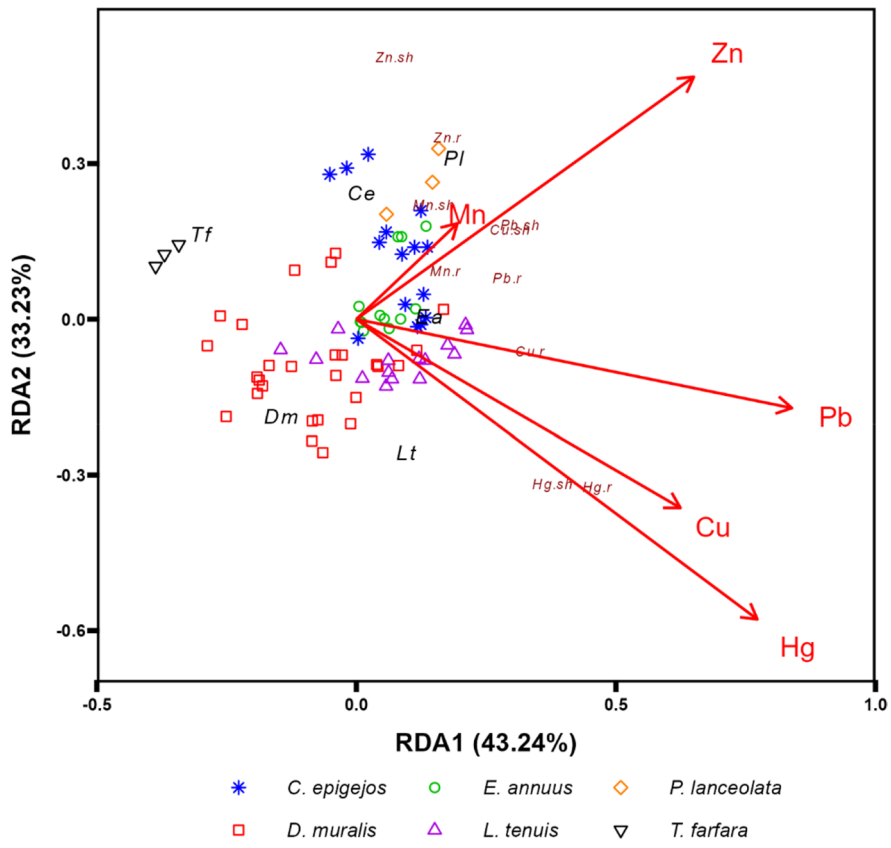

Fig. 6 Redundancy analysis (RDA) performed for the root and shoot metal concentrations and plant species distribution at the Turda, Romania site showing the first two RDA axis. Each red arrow denotes an environmental variable that significantly drives the observed plant community and plant elemental composition and corresponds to the rhizosphere soil metal concentrations. The response variables, metal root (r) and shoot (sh) concentrations are plotted in dark red, whereas plant species are pink (Ce = *Calamagrostis epigejos*, Dm = *Diplotaxis muralis*, Ea = *Erigeron annuus*, Lt = *Lotus tenuis*, Pl = *Plantago lanceolata*, Tf = *Tussilago farfara*)

Table 4 Environmental constraints (trace metal concentrations) and alpha biodiversity in the *Diplotaxis muralis*-associated rhizosphere soil samples at the Turda, Romania site

	mg kg^{-1} d.w.				ObservedOTUs	Shannon diversity index	PD-whole tree index	Chao1 diversity estimator	Simpson evenness index
	Hg	Pb	Cu	Zn					
T_1	128	155	214	121	904	7.6	54.7	934	1
T_2	228	363	798	513	859	7.8	52.0	921	1
T_3	346	125	204	184	582	6.9	39.1	603	1
T_4	615	403	364	370	658	7.6	43.8	683	1
T_5	302	90	86	218	173	5.0	17.7	279	0.9
T_6	265	152	271	317	850	8.2	51.9	891	1
Median	242	284	154	268	754	7.6	47.9	787	1

14%) and environmental information processing (mean 10%). However, the PCA on the KEGG pathways abundance data suggested a difference in the functional profile of the T_5 sample, by separating it from the other samples (Fig. 8B). The most abundant metabolism pathways putatively employed by the six microbial rhizosphere soil communities were carbohydrate and amino acid metabolisms with >15% mean relative abundance each, followed by energy metabolism with a mean relative abundance of 9% (Fig. 8A). The trend was mostly similar among the samples, with T_5 registering the minimum and the maximum value for the carbohydrate and the energy metabolism respectively. However, the differences between the extreme values were not far apart from the mean (low SE) (Fig. 8A). The most abundant

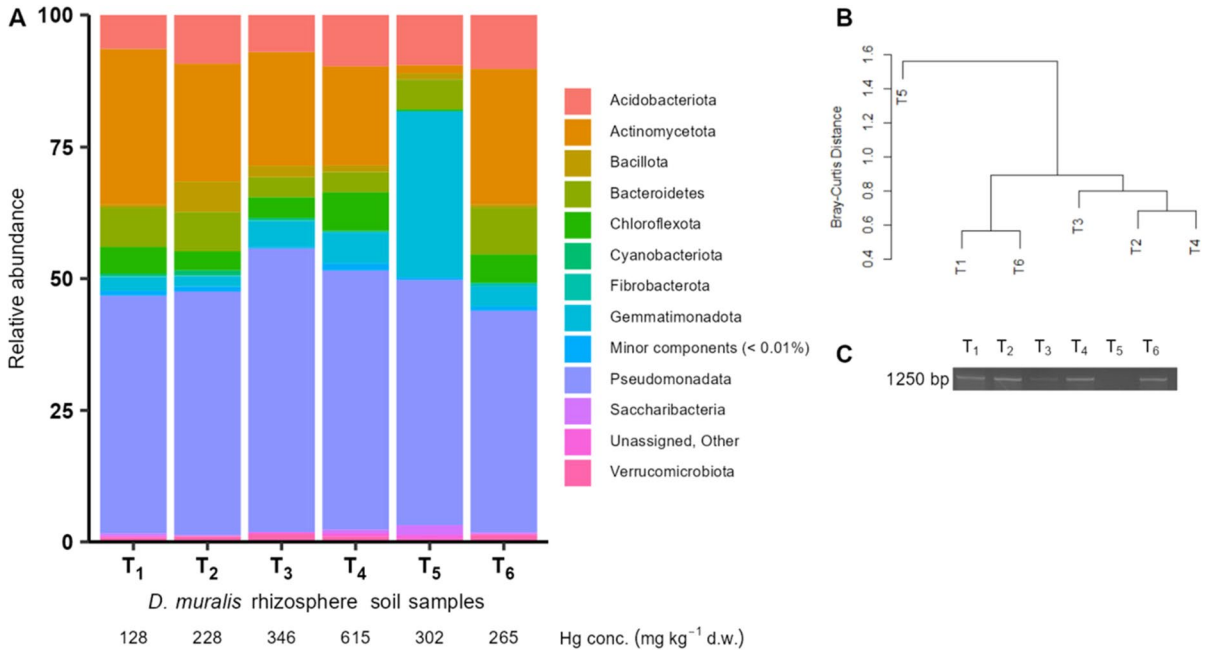

Fig. 7 The prokaryotic diversity and the presence of *merA* gene in the rhizosphere soil of *Diplotaxis muralis* plants, collected from each of the six subplots (T_1 to T_6) of the study site in Turda, Romania. The prokaryotic composition is shown as the relative abundance of taxa at the phylum level (**A**); the beta-diversity among the samples (**B**) was calculated based on Bray-Curtis dissimilarity distance, and the presence of the *merA* gene (**C**) in the prokaryotic communities is shown as a gel electrophoresis band at 1250 bp length

level 3 predicted KEGG pathway was for ABC transporters and had a relative abundance mean of 4.9%, the highest abundance (T_1) being 1.9 times higher than the minimum relative abundance (T_5) (Supplementary Fig. 3A). The next environmental information processing pathway with high relative abundance (mean 3%) was the two-component system pathway employed for signal transduction, where T_5 had the maximum relative abundance (3.5%).

Discussion

Plant species distribution and survival are influenced by a combination of both abiotic and biotic environmental factors (Dubuis et al. 2013; Pellissier et al. 2013). To assess the distribution of plant species at the Hg polymetallic-contaminated site studied herein, site-specific plant species and trace metal distribution, plant metal contents and the bacterial diversity within the rhizosphere of the dominant plant species were addressed.

The site was characterized by a high heterogeneity in trace metal distribution as seen from the large variation in the concentrations of the five trace metals selected as potential environmental drivers (Table 1). Rhizosphere soils were the most heterogeneous for Hg concentrations, with the maximum value being 79 times higher than the minimum, and the most homogeneous for Mn concentrations, with a median of 1149 mg kg^{-1} (Table 1). Soil Hg levels were alarmingly high at the site, with a median Hg concentration 96-fold higher than the intervention threshold for industrial sites (Table 1) (Ministerial Order No. 756/1997, 1997). Even the lowest measured soil Hg concentration at the site exceeded this threshold more than 3-fold. The median Cu and Pb concentrations in the rhizosphere soil surpassed the alert threshold for industrial soil by 1.05 and 1.4, respectively. The median concentrations of Mn and Zn were below legal alert limits. Furthermore, the potential ecological risk index (ERI) for the site, generated using the soil median concentrations of Hg, Pb, Cu, and Zn, was 769,745, 1000-fold higher than the threshold

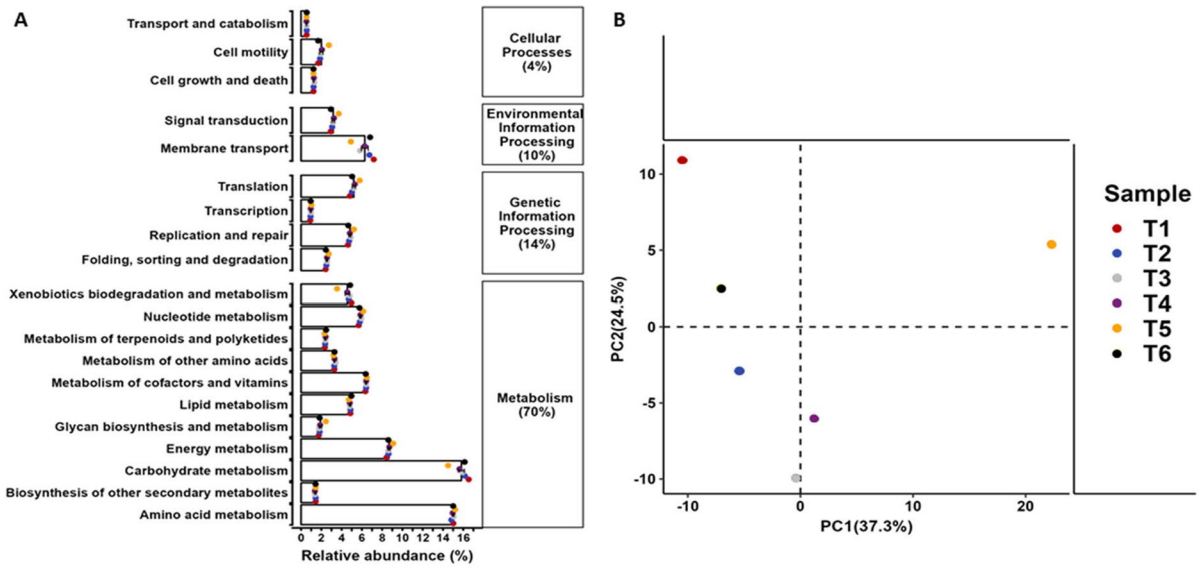

Fig. 8 Functional profiles inferred for the six rhizosphere soil microbiota samples from the Turda site, Romania. The mean relative abundance of predicted biological functions described according to the Kyoto Encyclopedia of Genes and Genomes (KEGG) pathway level 2 (left) and level 1 (right) (mean of n = 6 ± SE) (**A**); for figure simplification only the level 2 pathways are shown that have an >1% sum of relative abundance across the six samples. Principal component analysis (PCA) performed on the predicted KEGG abundance of biological functions highlighting differences in the variance of the microbial communities KEGG pathway abundance data (**B**)

for very high ecological risk, according to Hakanson (1980). Individually, there was a very low ecological risk for Cu, Pb, and Zn (52, 87.5, and 5.5, respectively, all <150), whereas the excessive degree of Hg pollution was reflected by an ERI of 769,600. Compared to global soil metal concentrations, Hg and Pb exceeded the median values 2405 and 14 times, respectively, whereas Cu, Zn, and Mn exceeded the median values 15, 6, and 3 times, respectively (Alloway 2013; Kabata-Pendias 2011; Salminen et al. 2005).

Therefore, Hg was hypothesized to be the major phytotoxic metal in the soil at the site and the main driver of plant community structure. Indeed, based on the RDA scores, soil Hg was the strongest driver of the observed variance at the site out of the five trace metals evaluated (Fig. 6). The Hg driven group of soil metals included Pb and Cu, and seemed to induce a plant (root and shoot) elemental status higher than the general plant sufficient levels (for Cu), compared to the second group observed which included soil Zn and Mn. Although the shoot Cu concentration in all six plant species reached or exceeded the general toxicity threshold of 20 mg kg^{-1} (Fig. 3C), there were no observable toxicity symptoms, whereas shoot Mn and Zn concentrations (Fig. 3) were generally not high enough to induce toxicity symptoms (Kabata-Pendias 2011). The Zn-Mn-driven group appears to confer a non-phytotoxic elemental composition throughout the plant tissues. Moreover, the potential presence of soil Mn oxides/ oxyhydroxides may have promoted the detainment of other essential macro- and micronutrients (Kabata-Pendias 2011; Singh and Schulze 2015). Alternatively, lower soil Hg concentrations corresponding to the soil that contained higher levels of Zn and Mn may have been sufficient for colonization by less Hg-tolerant plants.

Plants naturally found on highly metal-polluted soils often exhibit specific adaptations implementing a tolerance strategy, such as "excluder," "indicator," and "(hyper)accumulator" traits, as a result of edaphic selection pressure (Reeves et al. 2018). Excluders maintain low and constant levels of metals in shoot tissues across a wide range of metal concentrations in soil, shoot metal concentrations of indicators follow soil metal concentration in a linear manner, and (hyper)accumulators accumulate high metal concentrations in shoot across a broad range of metal

concentrations in soil (Baker 1981; Fernández et al. 2017). In situ metal contamination is heterogeneously distributed, thus a possible plant tolerance mechanism, especially for excluder species, is to avoid the metal uptake by developing the predominant part of their root system in the less contaminated patches of the soil (Golestanifard et al. 2020; Millis et al. 2004; Podar et al. 2004).

Diplotaxis muralis is an annual herbaceous plant of the cultivable "rocket" group of Brassicaceae, with a circum-Mediterranean geographic distribution and an ecology that includes semi-arid anthropogenic habitats (Bianco 1995). The substrate at the Turda site was rife in anthropogenic disturbance and Orthent soils consisting mainly of sand, which is a poor retainer of moisture (Petersen et al. 1968). *Diplotaxis muralis* has the lowest Ecological Indicator Value (EIV) for moisture (3.4) amongst the six plant species at the site, according to the European EIV database (Dengler et al. 2023), and thus the highest capabilities of colonizing dry soil patches. In the present study, the *D. muralis* population had the widest distribution at the site, growing on substrates spanning a broad range of Hg concentrations, which was also reflected in the patterns of Hg accumulation in roots and shoots (Fig. 3A). Moreover, these patterns exhibited strong positive linear relationships, as expected for an indicator plant (Fig. 5C). High Hg concentrations in roots and high BCF values, together with a low TF (Fig. 4A), suggested that *D. muralis* was efficient at immobilizing Hg in roots, and it could therefore promote a Hg phytostabilization process. Rocket plant species are known to accumulate nitrate (Signore et al. 2020). Soil nitrate could induce increased Hg uptake and alleviate root oxidative stress, as was seen in alfalfa plants (Carrasco-Gil et al. 2012), thereby suggesting a possible mechanism of Hg tolerance in *D. muralis*. Nitrate transporters (NRT), such as NRT1.1 can have low affinity for several metal cations, and can be involved in the simultaneous uptake of both metal ions and NO_3^-, as was shown for Cd (Mao et al. 2014). Moreover, the assimilation of nitrates can lead to the synthesis of glutamate, a precursor of phytochelatins, peptides involved in the sequestration of toxic elements (Forde and Lea 2007). Alternatively, it is possible that the rhizospheric bacterial community may confer a higher resilience to this plant species at this Hg-contaminated site (Fig. 7). Bacterial communities in the rhizosphere soil of *D. muralis* were generally highly diverse, without a significant Hg contamination-associated diversity loss (Table 4 and Fig. 7). It follows that the high soil Hg contamination has selected for microbial communities resistant to the principal contaminant, Hg, as highlighted by the presence of the *merA* gene in 5 of 6 rhizosphere bacterial communities (Fig. 7C).

The dominant bacteria in the rhizosphere of *D. muralis* plants align with the global soil bacteria atlas (Janssen 2006), with Pseudomonadota, Actinomycetota, and Acidobacteriota being the most prevalent (Fig. 7A). Moreover, results of the present study concur with those of Zheng et al. (2022), whereby Actinomycetota and Acidobacteriota were shown to increase in abundance in alkaline soils upon Hg addition. Solely, the T_5 sample had a relative abundance of Gemmatimonadota 16 times higher than the typical abundance in global soils (Delgado-Baquerizo et al. 2018). This phylum generally has a cosmopolitan distribution, based on its versatile metabolism (Mendez et al. 2008). However, its abundance in soil usually decreases with moisture, becoming a proxy for drier soils (DeBruyn et al. 2011). Moreover, Gemmatimonadota are thought to increase in abundance with long-term Hg contamination, albeit with an unknown mechanism (Liu et al. 2014).

In view of an in situ microorganism-assisted phytoremediation attempt, the few bacterial phylotypes identified at the genus level could be of interest. In this study, *Kaistobacter* was abundant in the rhizosphere of *D. muralis*. Previously, Liu et al. (2020) found *Kaistobacter* in high abundance among the bacterial communities in the rhizosphere soil of *Trifolium repens* growing in a Cd-contaminated soil. Furthermore, *Kaistobacter* was found associated with soils that suppress plant diseases caused by soil-borne pathogens (da R F Saraiva et al. 2020). The microbial communities of the *D. muralis* rhizosphere also had representatives from the groups that can act as plant growth-promoting rhizobacteria (Supplementary Fig. 2) (Hayat et al. 2010). Overall, the rhizosphere soil bacterial communities found here seemed to largely rely on harbouring the *merA* tolerance gene for survival. Through the mercuric reductase system, the microbiota in the rhizosphere of plants exposed to high soil Hg contamination could alleviate Hg stress on the plant roots, and thus facilitate colonization of the site.

The PICRUSt2 algorithm predicted that the main functions of the *D. muralis* rhizosphere soil communities of the Turda samples are largely involved in primary metabolic processes, suggesting a focus on growth and replication. This is common for rhizosphere soil communities as rhizosphere compartments are known to be sheltered niches for microbial growth where bacteria can benefit from plant metabolites (Hartmann et al. 2009). Similarly, metabolic processes accounted for half of the inferred functions within the rhizosphere communities of barley, tomato (Pii et al. 2016) and *Miscanthus* sp. (Chen et al. 2020). The metabolism of amino acids, carbohydrates and energy were the main subpathways of metabolism in this study, similar to the barley and tomato rhizosphere soil (Pii et al. 2016). Moreover, the presence of secondary metabolic pathways (xenobiotics biodegradation, other amino acids, terpenoids and polyketides metabolism, etc.) among the abundant metabolism pathways suggests there are also specialized functions in the microbial communities. Similar to the inferred functional profile of the rhizosphere microbiota of the energy crop, *Miscanthus* sp., genetic information processing and environmental information processing were the next main components of the functional profile of the Turda soil microbiota. The environmental information processing pathways (membrane transport and signal transduction) contain mechanisms of microbial adaptation to the environmental conditions, i.e. heavy metal stress. Not surprisingly, ABC transporters were the main components of the membrane transport pathway, similar to what Barra Caracciolo et al. (2020) and Fajardo et al. (2019) found for soil microbial communities exposed to heavy metal stress. In the membrane transport category, the pathways: phosphotransferase system (PTS), and bacterial secretion system were the most abundant in the T_5 soil sample, whereas the ABC transporters pathway was less abundant compared to all the other samples (Supplementary Fig. 3A). The PTS transporters actively uptake carbohydrates and are important in carbon metabolism and regulation (Xu et al. 2023). Bacterial secretion systems facilitate the transport of small molecules and proteins and through the interaction of the vast secretion system components promote bacterial survival, competition and virulence (Maphosa et al. 2023). Potentially, the T_5 soil microbiota rely on a strategy of colonizing the rhizosphere by adjusting the membrane transporters towards better metabolism regulation and more active competition mechanisms, as opposed to favoring transporters involved in metal metabolism. Moreover, within the ABC transporters subcategory, for the predicted genes with noticeable relative abundance (Supplementary Fig. 3B), there appears to be a recurring pattern of any one transporter being more abundant in T_5 opposed to all other samples, or less abundant than all other samples. This ping-pong pattern was however not present for the transporters involved in simple sugar (ABC.SS), iron complex transport system (ABC.FEV), and for the ABC-2A, the ATP binding protein of the ABC2 type transport system, suggesting a similarity in maintaining an effective transport for these types of vital molecules or the integrity of the ABC2 system. ABC systems catalyze the transport of diverse molecules, and potential ABC transporters mitigating metal resistance mechanisms were identified in members of Pseudomonadota phylum (Macur et al. 2001; Sá-Pereira et al. 2009), which was the most abundant phylum in the Turda rhizosphere communities.

Overall, through the PICRUSt2 analysis, two main strategies seem to be inferred for bacterial adaptation to the metal contamination in the rhizosphere soil. Due to the abundance of membrane transporters, it appeared that bacterial survival was a function of either potential metal resistance via ABC transporters or increased competitive strategies via secretion systems. It should be noted that certain important resistance and environmental adaptation mechanisms are typically found on plasmids (e.g. *mer* operon) and shared through lateral gene transfer in prokaryotes. Consequently, functional metagenome inferration methods are limited in providing a comprehensive understanding of the full metal resistance mechanism (Langille et al. 2013). To understand the relationships between Hg, plant roots, and rhizosphere microbiota, further studies are necessary to address the microbial diversity under a Hg gradient or as shaped by additional plant species as hosts.

Lotus tenuis is a perennial legume with tolerance to water deficiency, waterlogging, and highly saline environments (Escaray et al. 2012). It can tolerate high Na concentrations as a function of shoot Na exclusion (Teakle et al. 2006, 2007). Several halophytes are known to be able to develop additional tolerance to heavy metals, with root uptake, shoot accumulation and detoxification mechanisms enhanced under saline stress (Peng et al. 2022). In this study,

L. tenuis displayed positive correlations between the concentrations of Hg in soil and roots, soil and shoots, and roots and shoots, whereas for the other metals it had the lowest number of significant correlations, out of the plant species investigated (Table 3). *Lotus tenuis* could be an indicator for the most extreme level of soil Hg pollution, displaying the steepest slope of the linear regression of roots on soil Hg concentrations. *Lotus tenuis* was previously shown to be an indicator species for hexachlorocyclohexane (HCH) soil pollution (Balázs et al. 2018).

Calamagrostis epigejos is a perennial grass, the only monocot species investigated in this study. This population yielded a significant and positive correlation between shoots and soil Hg concentrations and can thus be considered a Hg indicator species. Compared with the other plant species investigated, *C. epigejos* had higher concentrations of trace metals (except Hg) in both roots and shoots. Actually, Cu, Zn, and Mn exceeded the threshold values for the mean adequate foliar concentrations by 5, 2.5, and 1.3 times, respectively (Van Der Ent and Baker 2013; Marschner 2012). This enrichment with micronutrients could indicate a potential response mechanism to the extreme Hg contamination of the soil. The increased Mn accumulation (root and shoot) compared to most of the other species of this study concurs with the findings of Esteban et al. (2013) on *Brassica napus*, who suggested that amelioration of Hg toxicity could be achieved by competitive uptake of Mn. Moreover, an efficient translocation of Mn to the aerial organs in different populations of *C. epigejos*, to the detriment of Pb, Cd, Zn, or Cu accumulation, was previously observed (Ranđelović et al. 2018). In this study, *C. epigejos* exhibited tolerance to phytotoxic rhizosphere soil concentrations of both Pb and Cu, in accordance with other studies (Lehmann and Rebele 2004a). Moreover, tolerance to Cd based on a root-level exclusion strategy has been previously investigated in pot experiments for *C. epigejos* (Lehmann and Rebele 2004b). Herein, Hg is added to the repertoire of possible metals tolerated by locally adapted populations of *C. epigejos*. Data herein also suggest that roots of *C. epigejos* became sinks for both micronutrient and non-micronutrient metals, promoting it as a phytostabilisation candidate for polymetallic-contaminated areas.

Erigeron annuus is an invasive annual plant, highly adaptable to anthropogenically disturbed lands due to its large genetic variation (Sennikov and Kurtto 2019). The Turda population of *E. annuus* showed only one significant Hg correlation, for soil-shoot concentration, but an overall limited Hg accumulation in shoots (low BAF, Fig. 4). Interestingly, *E. annuus* was the only investigated plant species that showed three significant linear regression relations with Pb, two negative (soil-to-root and root-to-shoot) and one positive (soil-to-shoot) (Table 3). The negative relationships seem to indicate an active root and shoot Pb exclusion mechanism, inferring a Pb excluder strategy in this population, however, the ecological risk index for Pb for the Turda site was very low (Hakanson 1980).

Plantago lanceolata and *T. farfara* are two perennial herbaceous weeds distinguished from the other plant species in the present study by their broader leaves and higher leaf-to-stem biomass ratios. The limited *P. lanceolata* population was present on the highest soil Zn concentrations, in accordance with other studies that reported populations of this species as tolerant Zn indicators (Leštan et al. 2003; Ahatović et al. 2020). This population was also growing on soil patches with high levels of Pb and Hg, and exhibited comparably high root-to-shoot translocation coefficients for both. Lead tolerance under edaphic pressure was in accordance with previous observations in *P. lanceolata* (Leštan et al. 2003). Unlike *P. lanceolata*, *T. farfara* was growing in soils of comparably lower Hg concentrations, and seemed to accumulate Hg exclusively in shoots; no detectable Hg was found in roots (Fig. 4). However, because of the small number of *P. lanceolata* and *T. farfara* individuals sampled, no confident relationships between tissue and soil Hg concentrations could be determined.

Plant Hg uptake and accumulation are complex processes that employ two distinct uptake routes. Soil-borne polar Hg species can be taken up by the root system, whereas airborne gaseous Hg species can be absorbed via stomata or adsorbed onto leaf tissues (Ericksen and Gustin 2004). In this study, both roots and shoots of all plant species had generally high Hg concentrations. The findings herein suggest that root and shoot Hg uptake is dependent not only on the soil Hg concentration, but also on the plant species (Fig. 5). Whereas most of the leaf adsorbed Hg dust was presumably removed from the shoots by washing, distinguishing between the two possible causes of shoot Hg accumulation remains elusive. Esbrí et al.

(2018) found that background soil Hg contamination at the Turda site greatly enriched the air with gaseous Hg, and this contamination spread proportionately farther from the source. Therefore, plant species at the site would be exposed to increased Hg levels in air. For *L. tenuis*, *D. muralis*, and *C. epigejos*, while both leaf uptake mechanisms could be feasible in theory, a common factor between these species are the significant correlations between Hg concentrations at all levels. Root and shoot Hg were dependent on soil Hg, and even shoot Hg was dependent on root Hg, suggesting a higher dependency on soil Hg and translocation for shoot Hg accumulation. However, *E. annuus*, a plant with an invasive colonization strategy, only correlated shoot Hg to soil Hg. Perhaps this difference in *E. annuus* compared to other species suggests a preference for one possible uptake mechanism e.g. foliar accumulation. Further experiments conducted under controlled conditions or reciprocal transplantation of plants in between non- or less contaminated and highly contaminated soil patches would be necessary to confirm this hypothesis.

Conclusions

The chlor-alkali plants utilizing Hg-cell technology significantly contributed to extensive Hg emissions, profoundly impacting the surrounding environment. The brownfield within the perimeter of the dismantled chlor-alkali plant in Turda, Romania, presents a very high ecological risk of Hg contamination, hindering any further use of the area. Despite the extreme Hg contamination, pioneer plants have colonized the site. These plants, along with the associated rhizosphere microbiome, could potentially be employed for nature-based phytomanagement of the contaminated area. A plant community survey conducted in this study identified six native herbaceous plant species, with *D. muralis* being the dominant one. High concentrations of mercury were detected in plant tissues, corresponding to significant levels of Hg in the soil. In the RDA model using soil trace metals as explanatory variables, *L. tenuis* and *D. muralis* emerged as the most promising species for growing on highly Hg-contaminated soil patches. Moreover, their high adaptive capacities to saline and dry soil, respectively, highlight their potential for phytoremediation of polymetallic-contaminated areas through phytostabilization. The third promising species was *C. epigejos,* another indicator of soil Hg-contamination. However, *E. annuus*, as abundant as *C. epigejos*, most-likely appeared at the site due to its invasive nature. Rare individuals of *P. lanceolata* and *T. farfara* were collected from soil patches with extreme Zn contamination or limited trace metal contamination, respectively. Due to the abundance at the site and the consequently low number of samples, no clear conclusions can be drawn for these two latter species. The survival of rhizosphere soil microbial communities was explained by the presence of the *merA* detoxification mechanism and likely a myriad of ABC transporters. Subsequently, this would assist plant growth through alleviating Hg stress. Thus, *D. muralis* and *L. tenuis* are proposed as candidate species for a phytomanagement attempt of the site, a strategy that must indispensably also incorporate resident microbial communities for maximal effectiveness.

Acknowledgments This work was supported by the Romanian National Authority for Scientific Research and Innovation, CNCS —UEFISCDI, project number PN-III-P2-2.1-PED-2019-5254, contract no. 390PED/2020. Emanuela D. Tiodar received a Short-Term Scientific Mission as part of CA19116 - Trace metal metabolism in plants, and a "Mittel- und Osteuropa (MOE)" Research Fellowship from Deutsche Bundesstiftung Umwelt, Germany. Cristian Coman was partially supported through the Core Project BIORESGREEN, subproject BioClimpact, number 7/30.12.2022. We would like to thank Diana Galea, Lavinia Ioana Fechete, and Daniel Cruceriu, for their help with soil and plant species processing. This article/publication is based upon work from COST Action CA19116 - PLANTMETALS, supported by COST (European Cooperation in Science and Technology).

Authors' contributions Conceptualization: DP, EDT, FP; Field sampling: DP, ZRB; Formal analysis and investigation: all; Writing - original draft preparation: ET; Writing - review and editing: all; Funding acquisition: DP, ET, UK; Resources: DP, MB, UK. Supervision: DP, MB, UK.

Funding This work was supported by the Romanian National Authority for Scientific Research and Innovation, CNCS — UEFISCDI, project number PN-III-P2-2.1-PED-2019-5254, contract no. 390PED/2020. Emanuela D. Tiodar received a Short-Term Scientific Mission as part of CA19116 - Trace metal metabolism in plants, and a "Mittel- und Osteuropa (MOE)" Research Fellowship from Deutsche Bundesstiftung Umwelt, Germany. Cristian Coman was partially supported through the Core Project BIORESGREEN, subproject BioClimpact, number 7/30.12.2022. This article/publication is based upon work from COST Action CA19116 - PLANTMETALS, supported by COST (European Cooperation in Science and Technology).

Data availability Sequence data generated in this study have been deposited in the European Nucleotide Archive (ENA) at EMBL-EBI under project accession numbers PRJEB67299.

Declarations

Competing interests The authors have no conflict of interest to declare. The authors have no relevant financial or non-financial interests to disclose.

References

Abadin H, Ashizawa A, Stevens Y-W, et al (2020) Toxicological profile for lead. Agency for Toxic Substances and Disease Registry (US). https://www.atsdr.cdc.gov/toxprofiles/tp13.pdf

Ahatović A, Čakar J, Subašić M, Hasanović M, Murtić S, Durmić-Pašić A (2020) *Plantago lanceolata* L. from serpentine soils in Central Bosnia tolerates high levels of heavy metals in soil. Water Air Soil Pollut 231. https://doi.org/10.1007/s11270-020-04561-7

Alloway BJ (2013) Heavy metals in soils, 3rd edn. Springer, Dordrecht

ATSDR (2005) Toxicological profile for zinc. U.S. Agency for Toxic Substances and Disease Registry, Atlanta. https://www.atsdr.cdc.goav/toxprofiles/tp60.pdf. Accessed 7.12.2022

ATSDR (2013) Toxicological profile for manganese. Agency for Toxic Substances and Disease Registry, Atlanta. https://www.atsdr.cdc.gov/toxprofiles/tp151.pdf. Accessed 7.12.2022

ATSDR (2022a) Toxicological profile for mercury (Draft for Public Comment). Agency for Toxic Substances and Disease Registry, Atlanta. https://www.atsdr.cdc.gov/toxprofiles/tp46.pdf . Accessed 7.12.2022

ATSDR (2022b) Toxicological profile for copper (Draft for Public Comment). U.S. Agency for Toxic Substances and Disease Registry, Atlanta. https://www.atsdr.cdc.gov/toxprofiles/tp132.pdf

Baker AJM (1981) Accumulators and excluders - strategies in the response of plants to heavy metals. J Plant Nutr 3:643–654. https://doi.org/10.1080/01904168109362867

Balázs HE, Schmid CAO, Feher I, Podar D, Szatmari PM, Marincaş O, Balázs ZR, Schröder P (2018) HCH phytoremediation potential of native plant species from a contaminated urban site in Turda, Romania. J Environ Manag 223:286–296. https://doi.org/10.1016/j.jenvman.2018.06.018

Barra Caracciolo A, Grenni P, Garbini GL, Rolando L, Campanale C, Aimola G, Fernandez-Lopez M, Fernandez-Gonzalez AJ, Villadas PJ, Ancona V (2020) Characterization of the belowground microbial community in a poplar-phytoremediation strategy of a multi-contaminated soil. Front Microbiol 11:2073. https://doi.org/10.3389/fmicb.2020.02073

Bianco V V (1995) Rocket, an ancient underutilized vegetable crop and its potential

Borcard ED, Gillet F, Legendre P (2012) Numerical Ecology with R. JABES 17:308–309. https://doi.org/10.1007/s13253-012-0094-x

Borymski S, Cycoń M, Beckmann M, Mur LAJ, Piotrowska-Seget Z (2018) Plant species and heavy metals affect biodiversity of microbial communities associated with metal-tolerant plants in metalliferous soils. Front Microbiol 9:1–18. https://doi.org/10.3389/fmicb.2018.01425

Braun-Blanquet J (1964) Pflanzensoziologie. Pflanzensoziologie. https://doi.org/10.1007/978-3-7091-8110-2

Carrasco-Gil S, Estebaranz-Yubero M, Medel-Cuesta D, Millán R, Hernández LE (2012) Influence of nitrate fertilization on hg uptake and oxidative stress parameters in alfalfa plants cultivated in a hg-polluted soil. Environ Exp Bot 75:16–24. https://doi.org/10.1016/j.envexpbot.2011.08.013

Chen Y, Tian W, Shao Y, Li YJ, Lin LA, Zhang YJ, Han H, Chen ZJ (2020) Miscanthus cultivation shapes rhizosphere microbial community structure and function as assessed by Illumina MiSeq sequencing combined with PICRUSt and FUNGUIld analyses. Arch Microbiol 202:1157–1171. https://doi.org/10.1007/s00203-020-01830-1

Chiriac CM, Szekeres E, Rudi K, Baricz A, Hegedus A, Dragoş N, Coman C (2017) Differences in temperature and water chemistry shape distinct diversity patterns in thermophilic microbial communities. Appl Environ Microbiol 83:1–20. https://doi.org/10.1128/AEM.01363-17

Cluj County Council (2012) Elaborarea Strategiei de Dezvoltare a Judeţului Cluj pentru perioada 2014–2020, Cod SMIS: 12836, Part III. https://cjcluj.ro/strategia-de-dezvoltare-a-judetului-cluj/. Accessed 15 Aug 2022

Cundy AB, Bardos RP, Puschenreiter M, Mench M, Bert V, Friesl-Hanl W, Müller I, Li XN, Weyens N, Witters N, Vangronsveld J (2016) Brownfields to green fields: Realising wider benefits from practical contaminant phytomanagement strategies. J Environ Manag 184:67–77. https://doi.org/10.1016/j.jenvman.2016.03.028

da R F Saraiva AL, da S Bhering A, do Carmo MGF, Andreote FD, Dias ACF, da S Coelho I (2020) Bacterial composition in brassica-cultivated soils with low and high severity of clubroot. J Phytopathol 168:613–619. https://doi.org/10.1111/jph.12941

DeBruyn JM, Nixon LT, Fawaz MN, Johnson AM, Radosevich M (2011) Global biogeography and quantitative seasonal dynamics of Gemmatimonadetes in soil. Appl Environ Microbiol 77:6295–6300. https://doi.org/10.1128/AEM.05005-11

Delgado-Baquerizo M, Oliverio AM, Brewer TE, Benavent-González A, Eldridge DJ, Bardgett RD, Maestre FT, Singh BK, Fierer N (2018) A global atlas of the dominant bacteria found in soil. Science (80-) 359:320–325. https://doi.org/10.1126/science.aap9516

Dengler J, Jansen F, Chusova O et al (2023) Ecological Indicator Values for Europe (EIVE) 1.0. Veg Classif Surv 4:7–29. https://doi.org/10.3897/VCS.98324

Dubuis A, Giovanettina S, Pellissier L, Pottier J, Vittoz P, Guisan A (2013) Improving the prediction of plant species distribution and community composition by adding edaphic to topo-climatic variables. J Veg Sci 24:593–606. https://doi.org/10.1111/jvs.12002

Ericksen J, Gustin M (2004) Foliar exchange of mercury as a function of soil and air mercury concentrations. Sci Total Environ 324:271–279. https://doi.org/10.1016/j.scitotenv.2003.10.034

Esbrí JM, Cacovean H, Higueras P (2018) Usage proposal of a common urban decorative tree (*Salix alba* L.) to monitor the dispersion of gaseous mercury: a case study from Turda (Romania). Chemosphere 193:74–81. https://doi.org/10.1016/j.chemosphere.2017.11.007

Escaray FJ, Menendez AB, Gárriz A, Pieckenstain FL, Estrella MJ, Castagno LN, Carrasco P, Sanjuán J, Ruiz OA (2012) Ecological and agronomic importance of the plant genus lotus. Its application in grassland sustainability and the amelioration of constrained and contaminated soils. Plant Sci 182:121–133. https://doi.org/10.1016/j.plantsci.2011.03.016

Esteban E, Deza MJ, Zornoza P (2013) Kinetics of mercury uptake by oilseed rape and white lupin: influence of Mn and cu. Acta Physiol Plant 35:2339–2344. https://doi.org/10.1007/s11738-013-1253-6

European Commission (2019) Communication from the commission to the European parliament, the European council, the council, the European economic and social committee and the committee of the regions The European Green Deal. https://eur-lex.europa.eu/legal-content/EN/TXT/HTML/?uri=CELEX:52019DC0640. Accessed 5 Dec 2022

European Commission (2020) Caring for soil is caring for life: ensure 75% of soils are healthy by 2030 for healthy food, people, nature and climate : interim report of the mission board for soil health and food. https://data.europa.eu/doi/10.2777/918775. Accessed 5 Dec 2022

Fajardo C, Costa G, Nande M, Botías P, García-Cantalejo J, Martín M (2019) Pb, cd, and Zn soil contamination: monitoring functional and structural impacts on the microbiome. Appl Soil Ecol 135:56–64. https://doi.org/10.1016/j.apsoil.2018.10.022

FAO (2022) Soils for nutrition: state of the art. https://doi.org/10.4060/cc0900en

Fernández S, Poschenrieder C, Marcenò C, Gallego JR, Jiménez-Gámez D, Bueno A, Afif E (2017) Phytoremediation capability of native plant species living on Pb-Zn and hg-as mining wastes in the Cantabrian range, north of Spain. J Geochemical Explor 174:10–20. https://doi.org/10.1016/j.gexplo.2016.05.015

Forde BG, Lea PJ (2007) Glutamate in plants: metabolism, regulation, and signalling. J Exp Bot 58:2339–2358. https://doi.org/10.1093/jxb/erm121

Frenţiu T, Ponta M, Sârbu C (2015) Prediction of the fate of hg and other contaminants in soil around a former chlor-alkali plant using fuzzy hierarchical cross-clustering approach. Chemosphere 138:96–103. https://doi.org/10.1016/j.chemosphere.2015.05.070

Frossard A, Donhauser J, Mestrot A, Gygax S, Bååth E, Frey B (2018) Long- and short-term effects of mercury pollution on the soil microbiome. Soil Biol Biochem 120:191–199. https://doi.org/10.1016/j.soilbio.2018.01.028

Garbisu C, Alkorta I, Kidd P, Epelde L, Mench M (2020) Keep and promote biodiversity at polluted sites under phytomanagement. Environ Sci Pollut Res 27:44820–44834. https://doi.org/10.1007/s11356-020-10854-5

Golestanifard A, Puschenreiter M, Aryan A, Santner J (2020) Metal accumulation and rhizosphere characteristics of *Noccaea rotundifolia* ssp. *cepaeifolia*. Environ Pollut 266:115088

Google Maps (2022) [Turda, Romania, Fostele fabrici Chimice]. Retrieved: September 26, 2022, from: https://www.google.com/maps/search/chemica+Turda/@46.5583311,23.7783133,355m/data=!3m1!1e3?entry=ttu

Gustin MS, Lindberg S, Marsik F et al (1999) Nevada STORMS project: measurement of mercury emissions from naturally enriched surfaces. J Geophys Res Atmos 104:21831–21844. https://doi.org/10.1029/1999JD900351

Hakanson L (1980) An ecological risk index for aquatic pollution control.A sedimentological approach. Water Res 14:975–1001. https://doi.org/10.1016/0043-1354(80)90143-8

Hartmann A, Schmid M, Tuinen DV, Berg G (2009) Plant-driven selection of microbes. Plant Soil 321:235–257. https://doi.org/10.1007/s11104-008-9814-y

Hayat R, Ali S, Amara U, Khalid R, Ahmed I (2010) Soil beneficial bacteria and their role in plant growth promotion: a review. Ann Microbiol 60:579–598. https://doi.org/10.1007/s13213-010-0117-1

Hornung RW, Reed LD (1990) Estimation of average concentration in the presence of nondetectable values. Appl Occup Environ Hyg 5:46–51

Janssen PH (2006) Identifying the dominant soil bacterial taxa in libraries of 16S rRNA and 16S rRNA genes. Appl Environ Microbiol 72:1719–1728. https://doi.org/10.1128/AEM.72.3.1719-1728.2006

Kabata-Pendias A (2011) Trace elements in soils and plants, 4th edn. Taylor and Francis Group, Boca Raton

Koch J, Chakraborty S, Li B, Moore Kucera J, Van Deventer P, Daniell A, Faul C, Man T, Pearson D, Duda B, Weindorf CA, Weindorf DC (2017) Proximal sensor analysis of mine tailings in South Africa: an exploratory study. J Geochemical Explor 181:45–57

Krausfeldt LE, Tang X, van de Kamp J, Gao G, Bodrossy L, Boyer GL, Wilhelm SW (2017) Spatial and temporal variability in the nitrogen cyclers of hypereutrophic Lake Taihu. FEMS Microbiol Ecol 93:24. https://doi.org/10.1093/femsec/fix024

Langille M, Zaneveld J, Caporaso J, McDonald D, Knights D, Reyes JA, Clemente JC, Burkepile DE, Vega Thurber RL, Knight R, Beiko RG (2013) Predictive functional profiling of microbial communities using 16S rRNA marker gene sequences. Nat Biotechnol 31:814–821. https://doi.org/10.1038/nbt.2676

Lehmann C, Rebele F (2004a) Evaluation of heavy metal tolerance in *Calamagrostis epigejos* and *Elymus repens* revealed copper tolerance in a copper smelter population of *C. Epigejos*. Environ Exp Bot 51:199–213. https://doi.org/10.1016/j.envexpbot.2003.10.002

Lehmann C, Rebele F (2004b) Assessing the potential for cadmium phytoremediation with *Calamagrostis epigejos*: a pot experiment. Int J Phytoremediation 6:169–183. https://doi.org/10.1080/16226510490454849

Leštan D, Grčman H, Zupan M, Bačac N (2003) Relationship of soil properties to fractionation of Pb and Zn in soil and their uptake into *Plantago lanceolata*. Soil Sediment Contam 12:507–522. https://doi.org/10.1080/713610986

Liu YR, He JZ, Zhang LM, Zheng YM (2012) Effects of long-term fertilization on the diversity of bacterial mercuric reductase gene in a Chinese upland soil. J Basic Microbiol 52:35–42. https://doi.org/10.1002/jobm.201100211

Liu YR, Wang JJ, Zheng YM, Zhang LM, He JZ (2014) Patterns of bacterial diversity along a long-term mercury-contaminated gradient in the Paddy soils. Microb Ecol 68:575–583. https://doi.org/10.1007/s00248-014-0430-5

Liu L, Li W, Song W, Guo M (2018) Remediation techniques for heavy metal-contaminated soils: principles and applicability. Sci Total Environ 633:206–219. https://doi.org/10.1016/j.scitotenv.2018.03.161

Liu C, Lin H, Li B, Dong Y, Yin T (2020) Responses of microbial communities and metabolic activities in the rhizosphere during phytoremediation of cd-contaminated soil. Ecotoxicol Environ Saf 202:110958. https://doi.org/10.1016/j.ecoenv.2020.110958

Macur RE, Wheeler JT, McDermott TR (2001) Microbial populations associated with the reduction and enhanced mobilization of arsenic in mine tailings. Environ Sci Technol 35(18):3676–3682. https://doi.org/10.1021/es0105461

Maghear I (2013) BILANT DE MEDIU Nivel I, SC CONSECVENT SRL, Turda, Cluj County, Romania

Mao QQ, Guan MY, Lu KX, Du ST, Fan SK, Ye YQ, Lin XY, Jin CW (2014) Inhibition of nitrate transporter 1.1-controlled nitrate uptake reduces cadmium uptake in Arabidopsis. Plant Physiol 166:934–944. https://doi.org/10.1104/pp.114.243766

Maphosa S, Moleleki LN, Motaung TE (2023) Bacterial secretion system functions: evidence of interactions and downstream implications. Microbiology 169(4):001326. https://doi.org/10.1099/mic.0.001326

Marschner H (2012) Marschner's mineral nutrition of higher plants. Edition No. 3

Mench MJ, Dellise M, Bes CM, Marchand L, Kolbas A, Le Coustumer P, Oustrière N (2018) Phytomanagement and remediation of cu-contaminated soils by high yielding crops at a former wood preservation site: sunflower biomass and ionome. Front Ecol Evol 6. https://doi.org/10.3389/fevo.2018.00123

Mendez MO, Neilson JW, Maier RM (2008) Characterization of a bacterial community in an abandoned semiarid lead-zinc mine tailing site. Appl Environ Microbiol 74:3899–3907. https://doi.org/10.1128/AEM.02883-07

Millis PR, Ramsey MH, John EA (2004) Heterogeneity of cadmium concentration in soil as a source of uncertainty in plant uptake and its implications for human health risk assessment. Sci Total Environ 326:49–53. https://doi.org/10.1016/j.scitotenv.2003.12.009

Ministerial Order No. 756/1997 (1997) Approving the regulation concerning the assessment of environmental pollution. (In Romanian). Off Gaz Part I, No 303bis/06111997

Ministry of Energy (2022) Strategia energetică a României 2022–2030, cu perspectiva anului 2050. https://energie.gov.ro/wp-content/uploads/2022/08/Strategia-2030_DGJRI_AM_12.08.2022_MU_Clean_25.08.2022-1.pdf. Accessed 17 Aug 2023

Mueller-Dombois D, Ellenberg H (1974) Aims and Methods of Vegetation Ecology. John Wiley and Sons, New York, p 547

Nies DH, Silver S (eds) (2007) Molecular microbiology of heavy metals (vol. 6). Springer Science & Business Media

Oksanen J, Blanchet FG, Friendly M et al (2017) Vegan: community ecology package. R package version 2.4--4.2. https://cran.r-project.org/package=vegan

Panagos P, Hiederer R, Van Liedekerke M, Bampa F (2013) Contaminated sites in Europe: review of the current situation based on data collected through a European network. Ecol Indic 24:439–450. https://doi.org/10.1016/j.ecolind.2012.07.020

Pellissier L, Pinto-Figueroa E, Niculita-Hirzel H, Moora M, Villard L, Goudet J, Guex N, Pagni M, Xenarios I, Sanders I, Guisan A (2013) Plant species distributions along environmental gradients: do belowground interactions with fungi matter? Front Plant Sci 4:1–9. https://doi.org/10.3389/fpls.2013.00500

Peng G, Lan W, Pan K (2022) Mechanisms of metal tolerance in halophytes: a Mini review. Bull Environ Contam Toxicol 109:671–683

Petersen GW, Cunningham RL, Matelski RP (1968) Moisture characteristics of Pennsylvania soils: I. Moisture retention as related to texture. Soil Sci Soc Am J 32:271–275

Pii Y, Borruso L, Brusetti L, Crecchio C, Cesco S, Mimmo T (2016) The interaction between iron nutrition, plant species and soil type shapes the rhizosphere microbiome. Plant Physiol Biochem 99:39–48. https://doi.org/10.1016/j.plaphy.2015.12.002

Podani J (2000) Introduction to the exploration of multivariate biological data. Backhuys Publishers

Podar D, Ramsey MH, Hutchings MJ (2004) Effect of cadmium, zinc and substrate heterogeneity on yield, shoot metal concentration and metal uptake by *Brassica juncea*: implications for human health risk assessment and phytoremediation. New Phytol 163:313–324. https://doi.org/10.1111/J.1469-8137.2004.01122.X

Popendorf KJ, Duhamel S (2015) Variable phosphorus uptake rates and allocation across microbial groups in the oligotrophic Gulf of Mexico. Environ Microbiol 17:3992–4006. https://doi.org/10.1111/1462-2920.12932

Prodan C, Micle V, Prodan MS (2011) Study on soil quality status in area of the former chemical plant from Turda and remediation proposals. ProEnvironment 4:259–263 https://journals.usamvcluj.ro/index.php/promediu/article/view/7861/6778

Ranđelović D, Jakovljević K, Mihailović N, Jovanović S (2018) Metal accumulation in populations of *Calamagrostis*

epigejos (L.) Roth from diverse anthropogenically degraded sites (SE Europe, Serbia). Environ Monit Assess 190. https://doi.org/10.1007/s10661-018-6514-9

R Core Team (2023). R: A Language and Environment for Statistical Computing. R Foundation for Statistical Computing, Vienna, Austria. https://www.R-project.org/

Reeves RD, Baker AJM, Jaffré T, Erskine PD, Echevarria G, van Der Ent A (2018) A global database for plants that hyperaccumulate metal and metalloid trace elements. New Phytol 218:407–411. https://doi.org/10.1111/nph.14907

Ronchi S, Salata S, Arcidiacono A, Piroli E, Montanarella L (2019) Policy instruments for soil protection among the EU member states: a comparative analysis. Land Use Policy 82:763–780. https://doi.org/10.1016/j.landusepol.2019.01.017

Ruiz-Huerta EA, Armienta-Hernández AM, Dubrovsky JG, Gómez-Bernal JM (2022) Bioaccumulation of heavy metals and as in maize (*Zea mays* L) grown close to mine tailings strongly impacts plant development. Ecotoxicology 31:447–467. https://doi.org/10.1007/s10646-022-02522-w

Salminen R, Batista MJ, Bidovec MD, et al (2005) Geochemical Atlas of Europe. Part 1 - Background Information, Methodology and Maps http://weppi.gtk.fi/publ/foregsatlas/map_compare.html. Accessed 13 Dec 2022

Sá-Pereira P, Rodrigues M, Simões F, Domingues L, Videira e Castro I (2009) Bacterial activity in heavy metals polluted soils: metal efflux systems in native rhizobial strains. Geomicrobiol J 26(4):281–288. https://doi.org/10.1080/01490450902892647

Sennikov AN, Kurtto A (2019) The taxonomy and invasion status assessment of *Erigeron annuus* s.l. (Asteraceae) in East Fennoscandia. Memoranda Societatis pro Fauna et Flora Fennica 95:40–59. Noudettu osoitteesta. https://journal.fi/msff/article/view/79497

Signore A, Bell L, Santamaria P, Wagstaff C, Van Labeke MC (2020) Red Light Is Effective in Reducing Nitrate Concentration in Rocket by Increasing Nitrate Reductase Activity, and Contributes to Increased Total Glucosinolates Content. Front Plant Sci 11. https://doi.org/10.3389/fpls.2020.00604

Singh B, Schulze DG (2015) Soil minerals and plant nutrition. Nat Educ Knowl 6:1. https://www.nature.com/scitable/knowledge/library/soil-minerals-and-plant-nutrition-127881474/. Accessed 23 Jan 2023

Sokal RR, Rohlf FJ (2012) Biometry. The principles and practice of statistics in biological research, 4th edn. W.H. Freeman and Company, New York

Szekeres E, Chiriac CM, Baricz A, Szőke-Nagy T, Lung I, Soran ML, Rudi K, Dragos N, Coman C (2018) Investigating antibiotics, antibiotic resistance genes, and microbial contaminants in groundwater in relation to the proximity of urban areas. Environ Pollut 236:734–744. https://doi.org/10.1016/j.envpol.2018.01.107

Taylor SR, McLennan SM (1995) The geochemical evolution of the continental crust. Rev Geophys 33:241–265. https://doi.org/10.1029/95RG00262

Tchounwou P, Yedjou C, Patlolla A, Sutton D (2012) Heavy metals toxicity and the environment. EXS 101:133–164. https://doi.org/10.1007/978-3-7643-8340-4_6

Teakle NL, Real D, Colmer TD (2006) Growth and ion relations in response to combined salinity and waterlogging in the perennial forage legumes *Lotus corniculatus* and *Lotus tenuis*. Plant Soil 289:369–383. https://doi.org/10.1007/s11104-006-9146-8

Teakle NL, Flowers TJ, Real D, Colmer TD (2007) *Lotus tenuis* tolerates the interactive effects of salinity and waterlogging by "excluding" Na+ and cl- from the xylem. J Exp Bot 58:2169–2180. https://doi.org/10.1093/jxb/erm102

Tiodar ED, Văcar CL, Podar D (2021) Phytoremediation and microorganisms-assisted phytoremediation of mercury-contaminated soils: challenges and perspectives. Int J Environ Res Public Health 18:1–38. https://doi.org/10.3390/ijerph18052435

Tóth G, Hermann T, Da Silva MR, Montanarella L (2016) Heavy metals in agricultural soils of the European Union with implications for food safety. Environ Int 88:299–309. https://doi.org/10.1016/j.envint.2015.12.017

United Nations (2023) The 17 goals. Available online at: https://sdgs.un.org/goals (verified 5 Sept 2023)

Văcar CL, Covaci E, Chakraborty S, Li B, Weindorf DC, Frențiu T, Pârvu M, Podar D (2021) Heavy metal-resistant filamentous Fungi as potential mercury Bioremediators. J Fungi 7:386. https://doi.org/10.3390/JOF7050386

Van Der Ent A, Baker AJM (2013) Hyperaccumulators of metal and metalloid trace elements: facts and fiction. 319–334. https://doi.org/10.1007/s11104-012-1287-3

Wang JJ, Ng TW, Zhang Q, Yang XB, Dahlgren RA, Chow AT, Wong PK (2012) Technical note: reactivity of C1 and C2 organohalogens formation - from plant litter to bacteria. Biogeosciences 9:3721–3727. https://doi.org/10.5194/bg-9-3721-2012

Weindorf DC, Chakraborty S (2020) Portable X-ray fluorescence spectrometry analysis of soils. Soil Sci Soc Am J 84:1384–1392

Xu T, Tao X, He H, Kempher ML, Zhang S, Liu X, Wang J, Wang D, Ning D, Pan C, Ge H (2023) Functional and structural diversification of incomplete phosphotransferase system in cellulose-degrading clostridia. ISME J 17(6):823–835. https://doi.org/10.1038/s41396-023-01392-2

Yang C, Mai J, Cao X, Burberry A, Cominelli F, Zhang L (2023) ggpicrust2: an R package for PICRUSt2 predicted functional profile analysis and visualization. Bioinformatics 39(8):btad470. https://doi.org/10.1093/bioinformatics/btad470

Zanganeh F, Heidari A, Sepehr A, Rohani A (2022) Bioaugmentation and bioaugmentation–assisted phytoremediation of heavy metal contaminated soil by a synergistic effect of cyanobacteria inoculation, biochar, and purslane (*Portulaca oleracea* L.). Environ Sci Pollut Res 29:6040–6059. https://doi.org/10.1007/s11356-021-16061-0

Zheng X, Cao H, Liu B, Zhang M, Zhang C, Chen P, Yang B (2022) Effects of mercury contamination on microbial diversity of different kinds of soil. Microorganisms 10. https://doi.org/10.3390/microorganisms10050977

Zuur AK, Ieno EN, Smith GM (2007) Analysing ecological data. In: Gail M, Kricketberg K, Samet J, WW TA (eds) Statistics for biology and health. Springer, New York